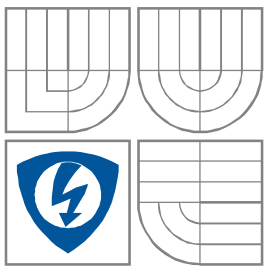


VYSOKÉ UČENÍ TECHNICKÉ V BRNĚ
BRNO UNIVERSITY OF TECHNOLOGY



FAKULTA ELEKTROTECHNIKY A KOMUNIKAČNÍCH
TECHNOLOGIÍ
ÚSTAV VÝKONOVÉ ELEKTROTECHNIKY
A ELEKTRONIKY
FACULTY OF ELECTRICAL ENGINEERING AND COMMUNICATION
DEPARTMENT OF POWER ELECTRICAL AND ELECTRONIC
ENGINEERING

***Model synchronního stroje s PM založeného na ekvivalentní
reluktanční síti***

***Model of a synchronous PM machine based on equivalent reluctance
network***

DIPLOMOVÁ PRÁCE

MASTER'S THESIS

AUTOR PRÁCE
AUTHOR

Bc. Peter Sporní

VEDOUCÍ PRÁCE
SUPERVISOR

doc. Ing. Čestmír Ondrůšek, CSc.

BRNO 2010



**BRNO UNIVERSITY
OF TECHNOLOGY**

**Faculty of Electrical Engineering
and Communication**

**Department of Power Electrical and Electronic
Engineering**

Diploma thesis

master's study field

Power Electrical and Electronic Engineering

Student: Peter Sporní, Bc.

ID: 78304

Year of study: 2

Academic year: 2009/10

TITLE OF THESIS:

**Model of a synchronous PM machine based on equivalent reluctance
network**

INSTRUCTIONS:

1. Provide the literature search.
2. Develop a model of synchronous PM machine and make a simulation.
3. Evaluate the results.

REFERENCE:

Assignment deadline: 1.10.2009

Submission deadline: 10.12.2009

Head of thesis: doc. Ing. Čestmír Ondrušek, CSc.

doc. Ing. Čestmír Ondrušek, CSc.

Subject Council chairman

WARNING:

The author of the semestral thesis must not in creating this thesis infringe the copyright of third parties, in particular, he must not infringe upon the rights of a foreign copyright personality in an illegal way and must be fully aware of the consequences of a breach of the provisions of Section 11 and Copyright Act No. 121/2000 Coll., including possible criminal consequences resulting from the provisions of Section 152 of Criminal Law No. 140/1961 Coll.

Abstract

This work disserts the problematics of creating and simulating reluctance network of the synchronous machine with V-shaped permanent magnets in the PSpice software. Firstly we familiarize with the construction and parameters of the machine and then we educt basic equations to calculate each component of the network. We calculate each component on the machine and then we create this network in PSpice. At the begining the simulated network is static and all magnetic resistivities are linear which gives us higher magnetic flux densities. Later we replace the steel sheets linear resistivities with nonlinear and we calculate also with working temperature of the permanent magnets. Then we compare our results with FEM method calculated values and we also calculate the induced voltage in one coil of winding. At the end we calculate power and torque characteristics of the machine.

Keywords

Synchronous machine, PM, reluctance, PSpice, magnetic flux, density, permeability, air gap, current, voltage, induced voltage, power, torque.

Anotácia

Táto práca pojednáva o problematike vytvárania a simulácie reluktančnej siete synchrónneho stroja s V tvarovanými permanentnými magnetmi v programe PSpice. Na začiatku sa oboznámime s konštrukciou a parametrami stroja a potom vyvodíme základné rovnice na výpočet každého prvku siete. Vypočítame každý prvak tohto stroja a potom vytvoríme túto sieť v PSpice. Na začiatku je simulovaná siet statická a všetky magnetické odpory sú lineárne. Neskôr nahradíme lineárne odpory reprezentujúce plechy nelineárnymi a počítame s precovnou teplotou permanentných magnetov. Potom porovnáme naše výsledky s FEM metódou počítanými hodnotami a vypočítame indukované napätie v jednej cievke stroja. Na záver vypočítame výkonovú a momentovú charakteristiku stroja.

Kľúčové slová

Synchrónny stroj, PM, reluktančná, PSpice, magnetický tok, indukcia, permeabilita, vzduchová medzera, prúd, napätie, indukované napätie, výkon, moment.

Bibliographic citation

SPORNI, P. *Model synchronního stroje s PM založeného na ekvivalentní reluktanční síti*. Brno: Vysoké učení technické v Brně, Fakulta elektrotechniky a komunikačních technologií, 2010. 53 s. Vedoucí diplomové práce doc. Ing. Čestmír Ondrušek, CSc.

Prehlásenie (Statement)

Prehlasujem, že svoju diplomovú prácu na tému „Model of a synchronous PM machine based on equivalent reluctance network“ som vypracoval samostatne pod vedením vedúceho semestrálneho projektu a s použitím odbornej literatúry a dalších informačných zdrojov, ktoré sú všetky citované v práci a uvedené v zoznamu literatúry na konci práce.

Ako autor uvedenej diplomovej práce ďalej prehlasujem, že v súvislosti s vytvorením tejto semestrálnej práce som neporušil autorské práva tretích osôb, predovšetkým som nezasiahol nedovoleným spôsobom do cudzích autorských práv osobnostných a som si plne vedomí následkov porušenia ustanovení § 11 a nasledujúcich autorského zákona č. 121/2000 Sb., vrátane možných trestnoprávnych dôsledkov vyplývajúcich z ustanovení § 152 trestného zákona č. 140/1961 Sb.

V Brne dňa Podpis autora

Acknowledgments

Thanks are due to doc. Ing. Čestmír Ondrušek, CSc. and Ing. Erik Odvarka for the motivation, professional help and hints in creating this work.



SUMMARY

INDEX OF FIGURES.....	2
INDEX OF TABLES.....	4
DEFINITION AND MEASURE OF USED SYMBOLS	5
INTRODUCTION.....	6
1 PARAMETERS OF PM MACHINE	7
1.1 WINDING.....	7
1.2 CONSTRUCTION.....	8
2 EDUCTION OF RECIPROCAL COMPONENTS OF MAGNETIC CIRCUIT	11
2.1 MAGNETIC CAPACITANCE/RELUCTANCE	11
2.2 COIL AS A SUPPLY OF MAGNETOMOTIVE FORCE	11
2.3 PERMANENT MAGNET AS A SUPPLY OF MAGNETOMOTIVE FORCE	12
3 CALCULATION OF RECIPROCAL COMPONENTS FOR STATIC MODEL IN PSPICE	14
3.1 STATOR COMPONENTS.....	14
3.2 AIR GAP COMPONENTS	19
3.3 ROTOR COMPONENTS	22
4 PSPICE SIMULATION RESULTS	25
4.1 MODEL WITHOUT WINDING CURRENT.....	25
4.2 MODEL WITH WINDING CURRENT.....	26
5 IMPROVING OF PSPICE MODEL.....	29
5.1 NONLINEAR RESISTORS	29
5.2 WORKING TEMPERATURE OF PM.....	32
5.3 ANGLE SHIFT OF ROTOR	32
6 FINAL PSPICE SIMULATION RESULTS.....	36
6.1 NO LOAD TEST	36
6.2 INDUCED VOLTAGE CALCULATION	37
6.3 POWER AND TORQUE CALCULATION	39
7 CONCLUSION.....	44
REFERENCES	45
ENCLOSURE	46



INDEX OF FIGURES

- Fig. 1. Placement of the coils in the winding.
Fig. 2. Blueprint of PM machine.
Fig. 3. Dimensions of the slots in the stator.
Fig. 4. Shape of the rotor pole in d-q axis.
Fig. 5. Equivalency of magnetic and electric circuit representing coil.
Fig. 6. Part of the simplified stator magnetic circuit.
Fig. 7. Equivalency of magnetic and electric circuit representing PM.
Fig. 8. Electric network representing magnetic reluctances of stator.
Fig. 9. Example of one segment.
Fig. 10. The real shapes of the stator segments.
Fig. 11. Phasor diagram of currents.
Fig. 12. Currents in the winding with their fluxpaths.
Fig. 13. Electric network representing magnetic reluctances of air gap.
Fig. 14. Electric network representing magnetic reluctances of rotor.
Fig. 15. The real shapes of the rotor segments.
Fig. 16. Section of network representing air gap over the pole without winding.
Fig. 17. Distribution of magnetic flux density over air gap without winding.
Fig. 18. Section of network representing air gap over the pole with winding.
Fig. 19. Distribution of magnetic flux density over air gap with winding.
Fig. 20. Distribution of magnetic flux density over air gap with changing current.
Fig. 21. GVALUE part connection.
Fig. 22. BH curve of the M235-35A steel inscribed to GVALUE part.
Fig. 23. GVALUE part representing R_{1x} .
Fig. 24. Nonlinear behavior of GVALUE part representing R_{1x} .
Fig. 25. Section of network over pole with nonlinear resistors.
Fig. 26. Magnetic flux density over air gap with nonlinear resistors with zero and nominal current in winding.
Fig. 27. Part of network with replaced air gap segments.
Fig. 28. One rotor segment connection.
Fig. 29. Changing of conductivity with angle.
Fig. 30. Part of the network with angle shift.



Fig. 31. Comparison of trapezium and cosinus change of conductivity.

Fig. 32. Distribution of magnetic flux density in the air gap during no load test (PSpice model).

Fig. 33. Distribution of magnetic flux density in the air gap during no load test (FEM calculation) [2].

Fig. 34. Change of magnetic flux through segments according to angle shift ($I=\Phi$).

Fig. 35. Average value of magnetic flux through one coil ($I=\Phi$).

Fig. 36. Shape of the u_i with trapezium change of conductivity in air gap.

Fig. 37. Induced voltage u_i .

Fig. 38. Reciprocal circuit of machine.

Fig. 39. Power characteristic of the synchronous machine according to load angle from first equation.

Fig. 40. Reciprocal circuits in d-q axis.

Fig. 41. Power characteristic of the synchronous machine according to load angle from second equation.

Fig. 42. Power characteristic of the synchronous machine according to load angle from both equations.

Fig. 43. Torque characteristic of the synchronous machine according to load angle from first equation.



INDEX OF TABLES

Table 1. Calculation of average airgap on selected ranges.



DEFINITION AND MEASURE OF USED SYMBOLS

B	-	magnetic flux density (T)
B_g	-	air gap magnetic flux density (T)
B_r	-	remanent magnetic flux density (T)
C_m	-	magnetic capacitance (H)
F_m	-	magnetic voltage (At)
F_{mA}	-	magnetic voltage created by phase A (At)
F_{mm}	-	magnetic voltage created by PM (At)
I	-	electric current (A)
M	-	torque (Nm)
N	-	number of coil turns (-)
P	-	power (W)
R_m	-	magnetic resistance (H^{-1})
R_a	-	phase resistance (Ω)
S	-	area (m^2)
U	-	electric voltage (V)
Z	-	impedance (Ω)
g	-	air gap (m)
i_m	-	magnetic current representing magnetic flux (Wb)
l	-	length (m)
pp	-	number of polepairs (-)
u_i	-	induced voltage (V)
β	-	load angle ($^\circ$)
Ψ	-	joint magnetic flux (Wb)
Ψ_{PM}	-	flux linkage due to permanent magnets (Wb)
Φ	-	magnetic flux (Wb)
θ	-	angle ($^\circ$)
μ_r	-	relative permeability (-)
ω	-	angular velocity (rad^{-1})



INTRODUCTION

This work is about creating a simulation model of synchronous machine with V-shaped permanent magnets and was created on request of Cummins Inc.. At the begining we would like to explain why is this type of machine so important. This type of electric machine is todays mostly used type in the hybrid personal cars which are more enviromental friendly because of their lower oil consumption and emissions. Synchronous machine is used because of its good control properties and the modern permanent magnets, which are V-shaped, enable to remove the rotor winding of machine which connection to supply is unreliable. So there is a big effort of industry to design more efficient and stronger machines of this construction to enable their wider use in different kinds of vehicles.

For the simulation we are using capacitance/reluctance network instead of analytical methods based on Laplace or Poisson equations. These methods are used for machines with surface mounted PM which behaves lineary. But because of the V-shaped PMs and nonlinear bridges holding the magnets in the rotor these methods can not be used in our case. The result of our work will be dynamic model of this machine with nonlinear magnetic resistors representing steel sheets.



1 PARAMETERS OF PM MACHINE

1.1 Winding

The main parameters of given PM machine are listed below.

Embedded-PM 45kW@1300rpm

Field weakening up to 2500rpm,

Pmax=90kW

48 slots, 8 poles

Laminations: M235-35A steel

Magnet grade: NdFeB N38EH @ 70degC

Tooth width is constant

Slot fill factor = 48%

Axial length=200mm

Winding parameters: (lap winding)

No of parallel paths: 4

Turns in series: 22

No of layers in a slot: 1

Wires in hand: 6

Wire dia: 0.95mm

Chording: full pitch

Nominal winding temperature: 160degC

Nominal current: 203.7 Arms

Nominal supply voltage: 102Vrms,phase

Placement of the coils in the winding of machine can be seen in Fig. 1.. It displays only 12 slots which are repeating periodically in all of the 48 slots of machine. A is beginning and A_0 is the end of the coil. In the work we assume that the ends are connected so it is star connection machine. Current flowing through one coil of one phase is one quarter of nominal current because of the number of parallel paths.

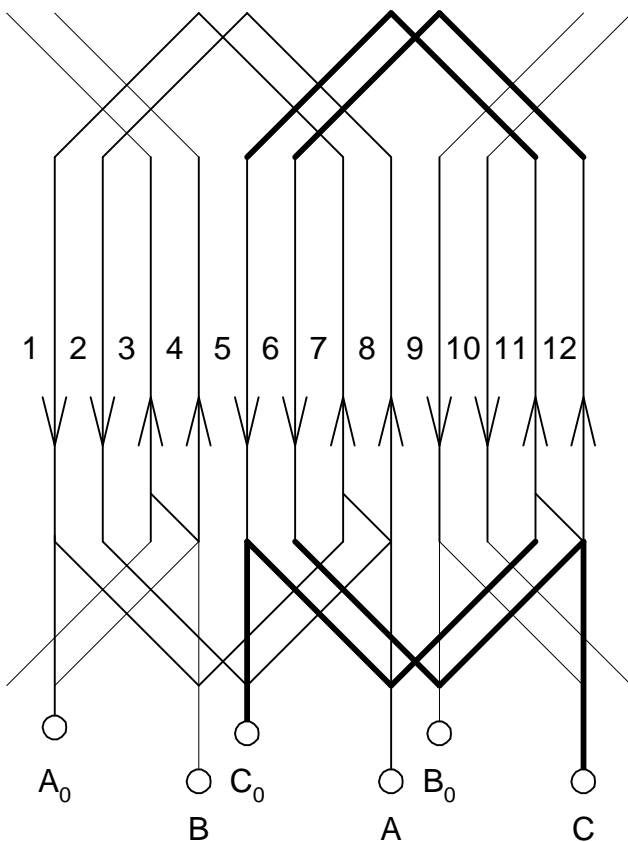


Fig. 1. Placement of the coils in the winding.

1.2 Construction

The construction of PM machine can be seen on following pictures (Fig. 2., Fig. 3.). Shape of the poles on the rotor of machine is very specific and it is defined in the d-q axis in electrical degrees by function:

$$g = \frac{g_{min}}{\cos\vartheta} ; \vartheta \in <0; 72^\circ>; g_{min} = 1.15mm \quad (1.1)$$

And it is linear on the interval:

$$\vartheta \in <72^\circ; 90^\circ>; g(72^\circ) = 3.72mm; g(90^\circ) = 6.44mm \quad (1.2)$$

This shape is displayed in the picture 4.. When we want to know the shape in the real degrees we only need to divide the degrees in the Fig. 4. on the axis x by 4.

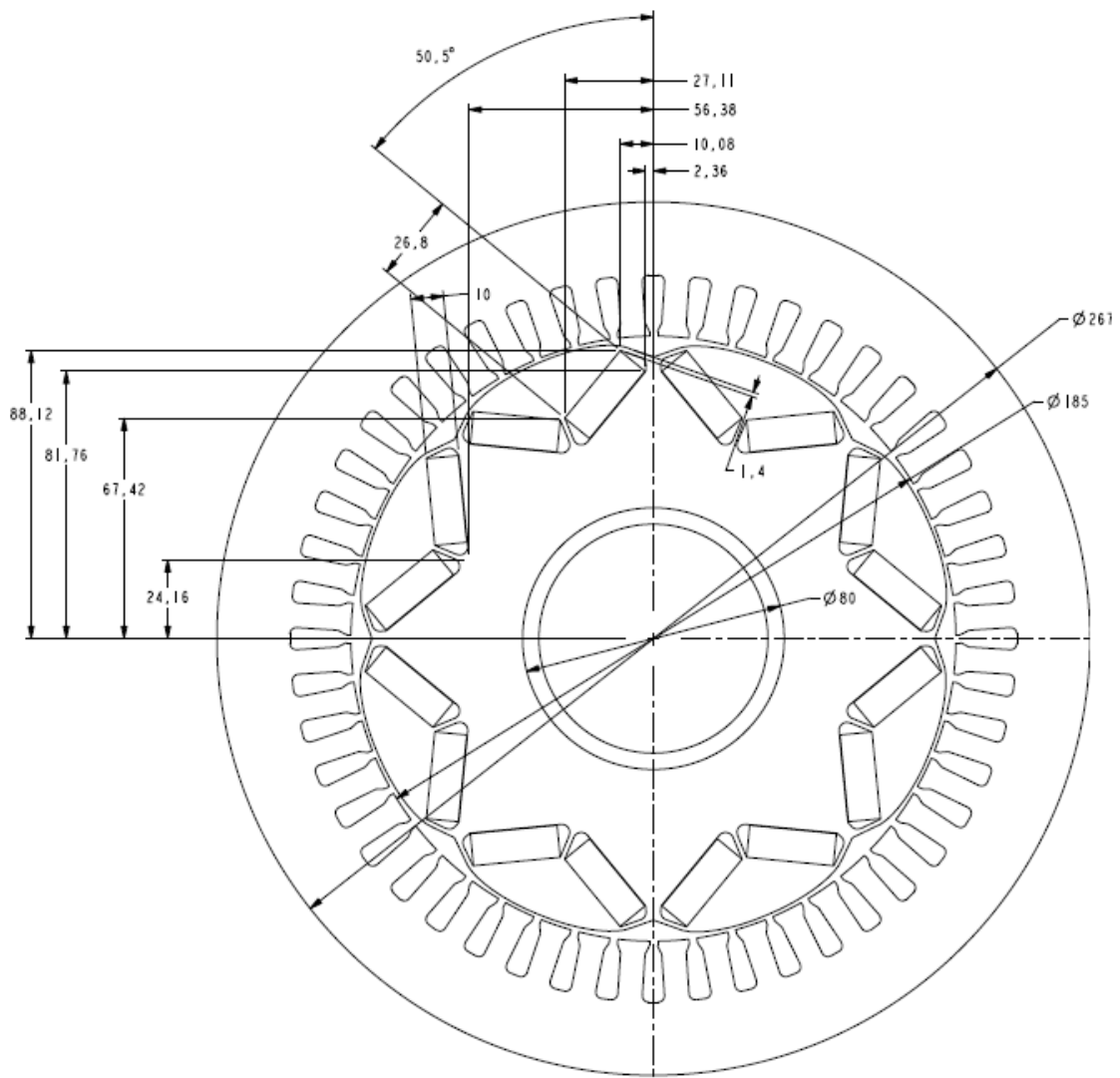


Fig. 2. Blueprint of PM machine.

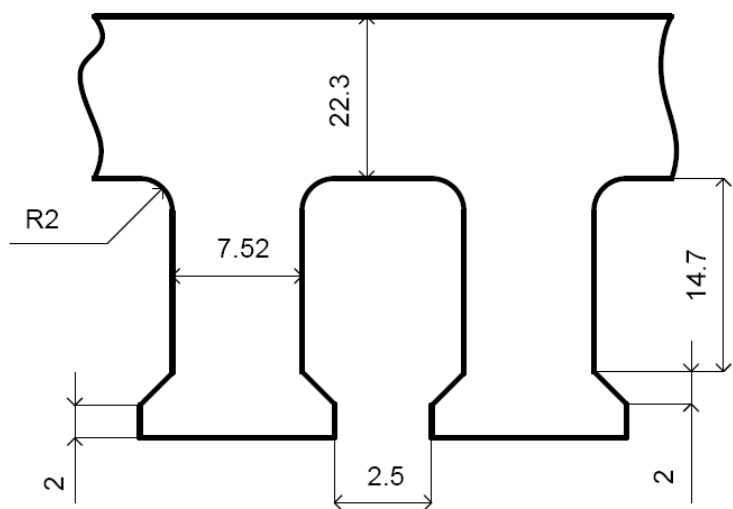


Fig. 3. Dimensions of the slots in the stator.

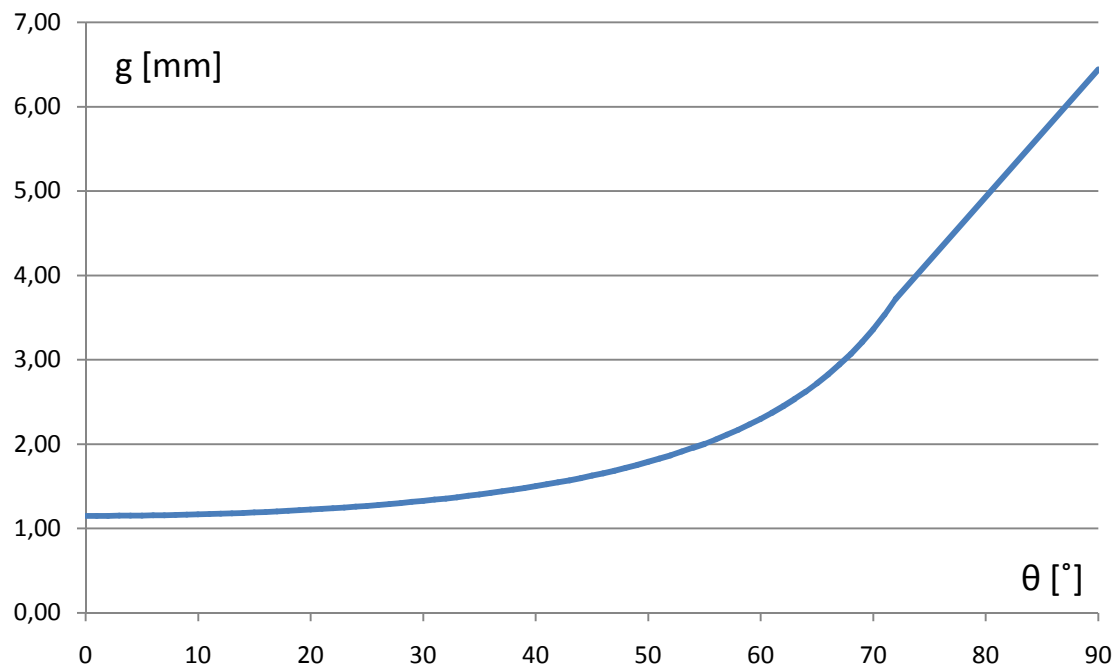


Fig. 4. Shape of the rotor pole in d - q axis.



2 EDUCTION OF RECIPROCAL COMPONENTS OF MAGNETIC CIRCUIT

2.1 Magnetic capacitance/reluctance

The magnetic capacitor corresponding to article [4] is defined:

$$C_m = \frac{1}{R_m} = \frac{\mu_0 \mu_r}{l} S \quad (2.1)$$

The magnetic capacitance is defined as the reciprocal of a pure magnetic reluctance. The advantages over the more usual representation of magnetic reluctances as resistors in magnetic circuits, and therefore energy dissipative instead of energy storing are obvious, and for pure reluctances the following magnetic circuit relationships which are immediately analogues to the corresponding electric circuit relationships, amongst other too numerous to state here, follow naturally: [3]

$$i_m = \frac{d\phi}{dt} = \frac{dq_m}{dt} \quad (2.2)$$

$$i_m = C_m \frac{dF_m}{dt} \quad (2.3)$$

$$F_m = \frac{1}{C_m} \int i_m dt = R_m \int i_m dt \quad (2.4)$$

However later in this work we realized that placing a capacitor in the PSpice electric model of the magnetic circuit of machine gives hardly evaluable results and it brings more problems than it solves. So in the PSpice electric model we are using resistors instead of capacitors and we are still using the equations 2.1-2.4 because the magnetic capacitance is defined as the reciprocal of magnetic reluctance. In short we are using well known Ohm-Hopkins law equivalency.

2.2 Coil as a supply of magnetomotive force

The amount of magnetomotive force supplied by a coil to a magnetic circuit is defined:

$$F_m = NI \quad (2.5)$$

N- number of turns of coil

I- electric current flowing thru the coil

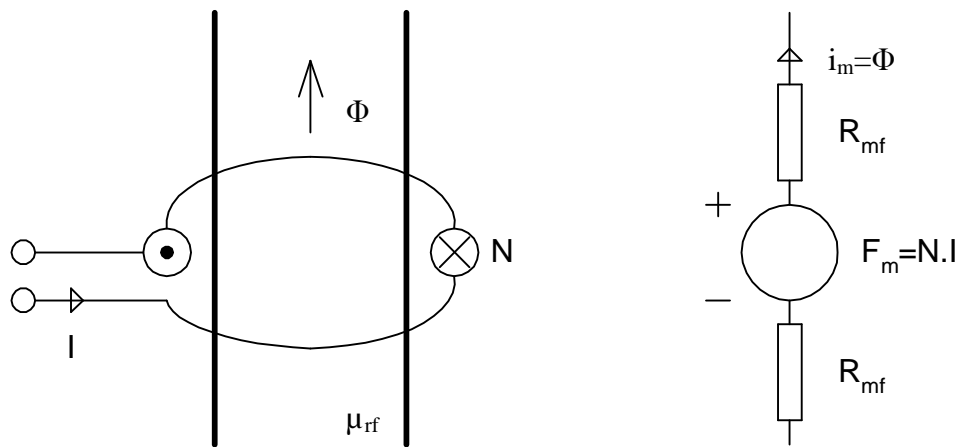


Fig. 5. Equivalency of magnetic and electric circuit representing coil.

But in the stator of electric machines the coil is placed in the slots that are not near each other so we need to define magnetic voltage created by a number of conductors placed in one slot respectively in our case, half of the coil:

$$F_m = \frac{NI}{2} \quad (2.6)$$

N- number of conductors in a slot

I- electric current flowing thru the coil

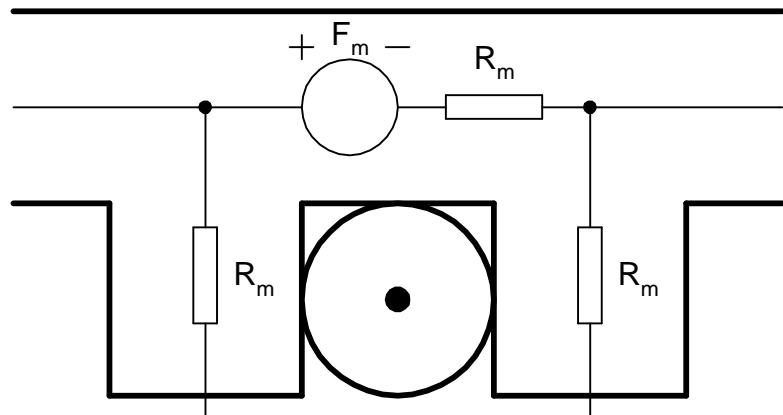


Fig. 6. Part of the simplified stator magnetic circuit.

2.3 Permanent magnet as a supply of magnetomotive force

Permanent magnet in magnetic circuit can be represented by a voltage supply with a reluctance representing its magnetic resistivity. The magnetomotive force can be easily derived:

$$\phi = B_r S \quad (2.7)$$

$$F_m = \phi \cdot R_m = \phi = B_r \cdot S \frac{l}{\mu_0 \mu_r S} \quad (2.8)$$

$$F_m = \frac{B_r l}{\mu_0 \mu_r} \quad (2.9)$$

B_r - remanent magnetic flux density of PM

l - thickness of PM

μ_r - relative permeability of PM

R_m – resistivity of PM

R_{mf} – resistivity of ferrum core

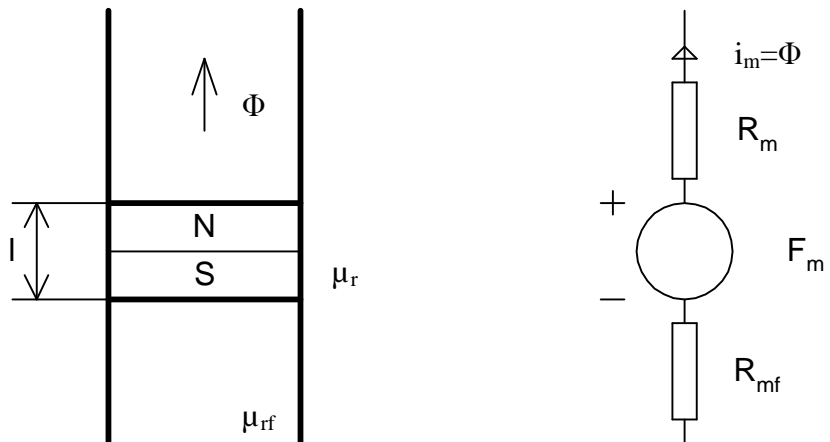


Fig. 7. Equivalency of magnetic and electric circuit representing PM.

3 CALCULATION OF RECIPROCAL COMPONENTS FOR STATIC MODEL IN PSPICE

3.1 Stator components

In the process of calculating the reciprocal components of machine we divided its area into segments. Each of this component consists of a node and four resistors. In the case of winding and PM components they consist of additional two voltage supplies. We can see the real PSpice electric network representing part of stator in Fig. 8..

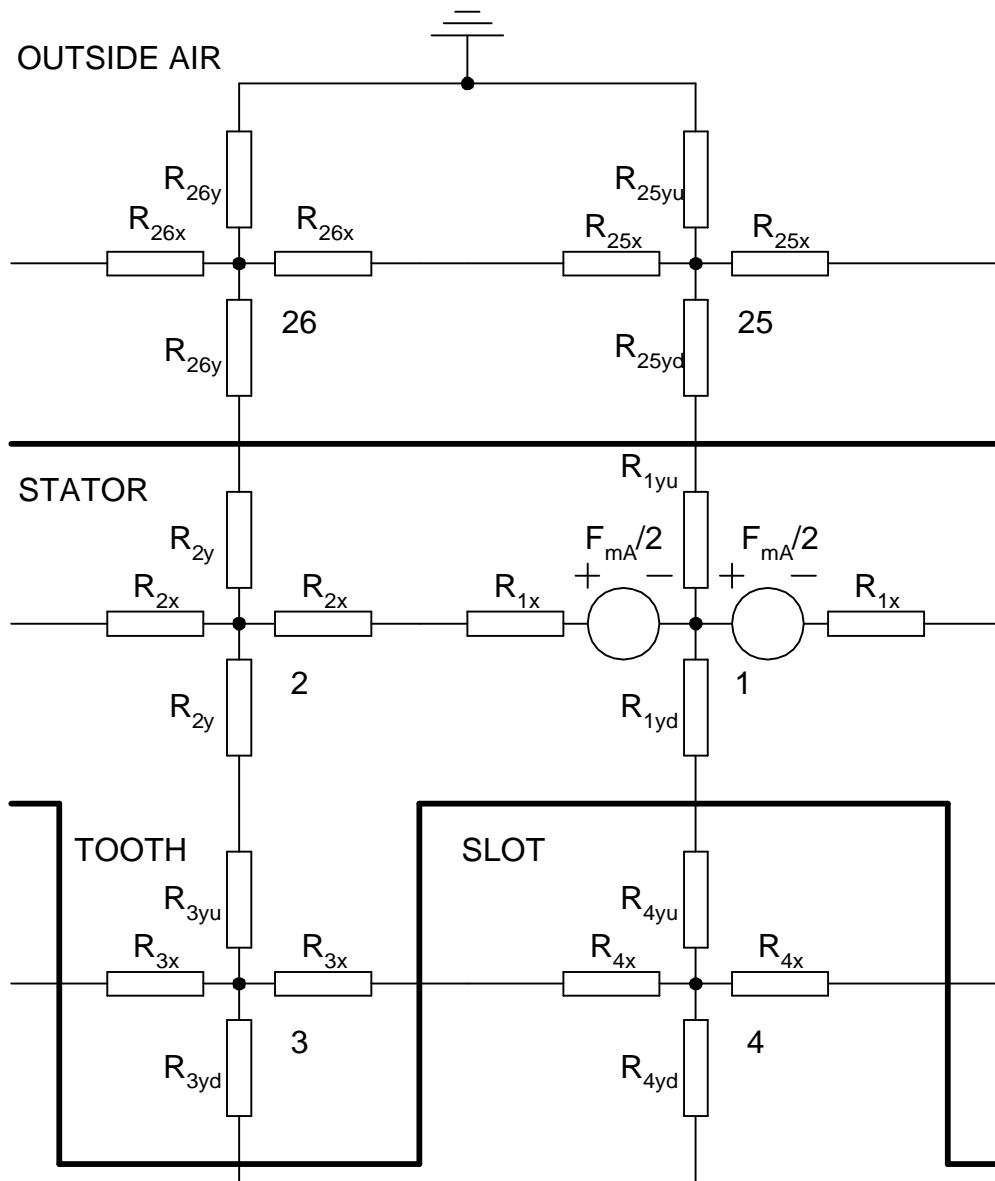


Fig. 8. Electric network representing magnetic reluctances of stator.

The resistors are calculated with this equation:

$$R_m = \frac{l}{\mu_0 \mu_r s} \quad (3.1)$$

l - half length of segment in the direction perpendicular to the area S of the resistor we are calculating

S - area of segment that is perpendicular to the current (magnetic flux) flow of the resistor we are calculating

μ_r – relative permittivity of the material which is the resistor representing

Example of calculating resistors in one segment:

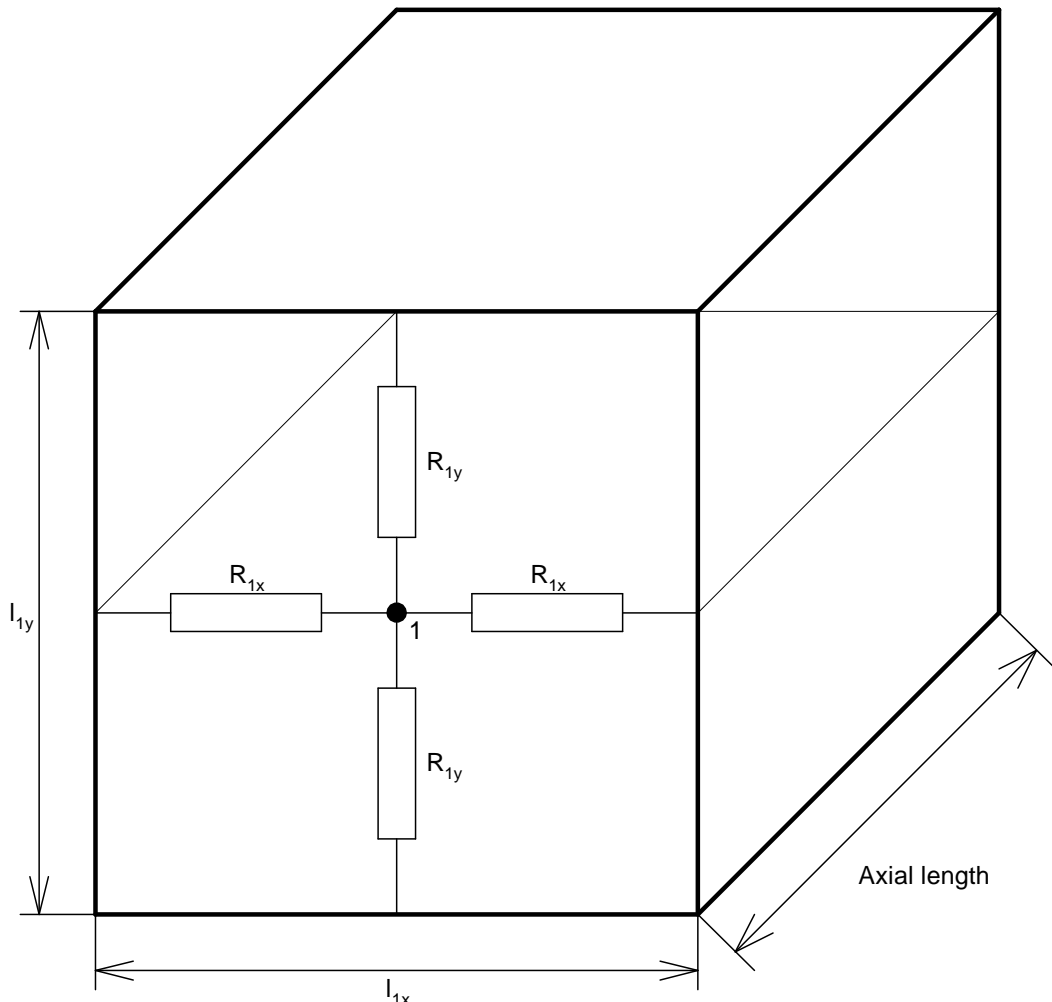


Fig. 9. Example of one segment.

$$R_{1x} = \frac{l_{1x}/2}{\mu_0 \mu_r l_{1y} \cdot a}$$

$$R_{1y} = \frac{l_{1y}/2}{\mu_0 \mu_r l_{1x} \cdot a}$$

a – Axial length

The exact sizes of lengths and areas of each segment were obtained from Autodesk Inventor blueprint of the machine (Fig. 9.). For the brief description not all sizes are visualized.

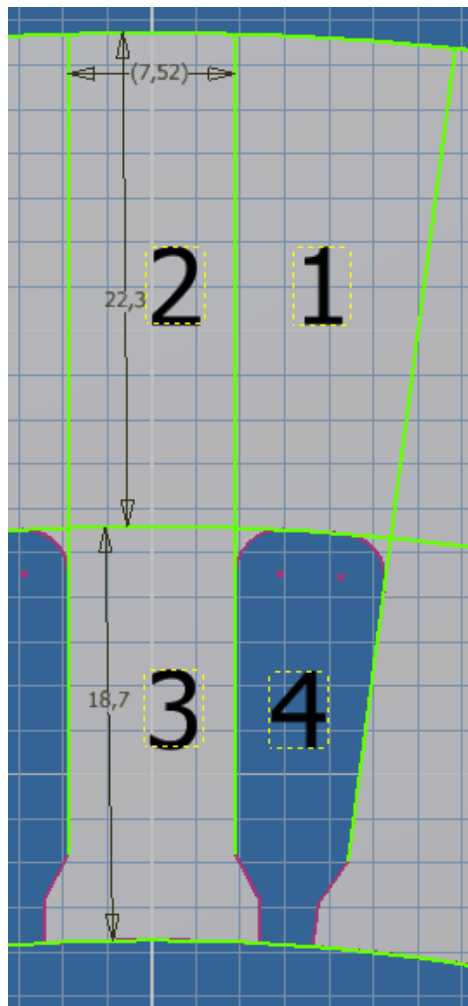


Fig. 10. The real shapes of the stator segments.

As we can see on Fig. 10. the segments are horizontally equal so the R_x resistors of each segment will be same, but some segments have different areas in longitudinal direction on their upper and down side so the R_{yu} and R_{yd} resistors will be different.

Calculation of stator resistors:

Relative permitivity of electrical steel: $\mu_r=2000$

Length of machine: 200mm

$$S_{1x}=22.3 \cdot 200 = 4460 \text{ mm}^2$$

$$l_{1x}=8.494/2= 4.247 \text{ mm}$$

$$R_{1x} = \frac{4.247 \cdot 10^{-3}}{\mu_0 \cdot 2000 \cdot 4460 \cdot 10^{-6}} = 378.9 \text{ H}^{-1}$$

$$S_{1yu}=9.224 \cdot 200= 1844 \text{ mm}^2$$

$$l_{1y}=11.5 \text{ mm}$$

$$R_{1yu} = \frac{11.5 \cdot 10^{-3}}{\mu_0 \cdot 2000 \cdot 1844 \cdot 10^{-6}} = 2481.4 \text{ H}^{-1}$$



$$S_{1yd} = 7.765 * 200 = 1552.9 \text{ mm}^2$$

$$R_{1yd} = \frac{11.5 * 10^{-3}}{\mu_0 * 2000 * 1552.9 * 10^{-6}} = 2946 \text{ H}^{-1}$$

$$S_{2x} = 22.3 * 200 = 4460 \text{ mm}^2$$

$$l_{2x} = 7.521 / 2 = 3.76 \text{ mm}$$

$$R_{2x} = \frac{3.76 * 10^{-3}}{\mu_0 * 2000 * 4460 * 10^{-6}} = 335.5 \text{ H}^{-1}$$

$$S_{2y} = 7.521 * 200 = 1504.2 \text{ mm}^2$$

$$l_{2y} = 22.3 / 2 = 11.5 \text{ mm}$$

$$R_{2y} = 3041.95 \text{ H}^{-1}$$

$$S_{3x} = (3.247 + 12.621 + 2.318 + 2) * 200 = 4037.2 \text{ mm}^2$$

$$l_{3x} = 7.868 / 2 = 3.934 \text{ mm}$$

$$R_{3x} = 387.7 \text{ H}^{-1}$$

$$S_{3yu} = 7.52 * 200 = 1504 \text{ mm}^2$$

$$l_{3y} = 9.35 \text{ mm}$$

$$R_{3yu} = 2473.6 \text{ H}^{-1}$$

$$S_{3yd} = 8.214 * 200 = 1643 \text{ mm}^2$$

$$R_{3yd} = 2264.3 \text{ H}^{-1}$$

$$S_{4x} = (3.247 + 12.621 + 2.318 + 2) * 200 = 4037.2 \text{ mm}^2$$

$$l_{4x} = 5.81 / 2 = 2.905 \text{ mm}$$

$$R_{4x} = \frac{2.905 * 10^{-3}}{\mu_0 * 4037.2 * 10^{-6}} = 572.6 \text{ kH}^{-1}$$

$$S_{4yu} = 6.423 * 200 = 1284.5 \text{ mm}^2$$

$$l_{4y} = 9.35 \text{ mm}$$

$$R_{4yu} = 5792.5 \text{ kH}^{-1}$$

$$S_{4yd} = 4.5 * 200 = 900 \text{ mm}^2$$

$$R_{4yd} = 8267.2 \text{ kH}^{-1}$$

$$S_{25x} = 22.3 * 200 = 4460 \text{ mm}^2$$

$$l_{25x} = 11.414 / 2 = 5.707 \text{ mm}$$

$$R_{25x} = \frac{5.707 * 10^{-3}}{\mu_0 * 4460 * 10^{-6}} = 1018.3 \text{ kH}^{-1}$$

$$S_{25yu} = 12.14 * 200 = 2428 \text{ mm}^2$$

$$l_{25y} = 22.3 / 2 = 11.15 \text{ mm}$$

$$R_{25yu} = 3654.4 \text{ kH}^{-1}$$

$$S_{25yd} = 10.683 * 200 = 2136.6 \text{ mm}^2$$



$$R_{25yd} = 4152.8 \text{ kH}^{-1}$$

$$S_{26x} = 22.3 * 200 = 4460 \text{ mm}^2$$

$$l_{26x} = 7.521 / 2 = 3.76 \text{ mm}$$

$$R_{26x} = \frac{3.76 * 10^{-3}}{\mu_0 * 4460 * 10^{-6}} = 671 \text{ kH}^{-1}$$

$$S_{26yu} = 7.521 * 200 = 1504.2 \text{ mm}^2$$

$$l_{26y} = 22.3 / 2 = 11.15 \text{ mm}$$

$$R_{26y} = 5898.7 \text{ kH}^{-1}$$

Calculation of magnetic voltage generated by slot of winding:

If the nominal current of machine is 203.7Arms and number of parallel paths is 4 then the current flowing thru the coil would be 50.925Arms. Because we are making static model $I_{A,pk}$ current will flow only by the phase A. The current in the other phases will be according to phasor diagram in Fig. 11..

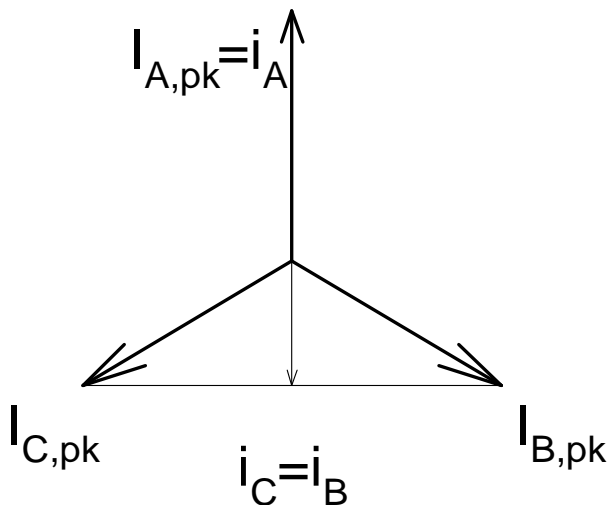


Fig. 11. Phasor diagram of currents.

$$I_{A,pk} = I_{A,rms} \sqrt{2} = 50.925 \cdot \sqrt{2} = 70.02 \text{ A}$$

$$I_{A,pk} = I_{B,pk} = I_{C,pk}$$

$$i_A = I_{A,pk} \sin\left(\frac{\pi}{2}\right) = 1 \cdot I_{A,pk} = 70.02 \text{ A}$$

$$i_B = I_{B,pk} \sin\left(\frac{\pi}{2} + \frac{2}{3}\pi\right) = -0.5 * I_{B,pk} = -35.01 \text{ A}$$

$$i_C = I_{C,pk} \sin\left(\frac{\pi}{2} + \frac{4}{3}\pi\right) = -0.5 * I_{C,pk} = -35.01 \text{ A}$$



Then the voltage generated by winding in a slot will be according to equation 2.6:

$$F_{mA} = \frac{Ni_A}{2} = \frac{22*70.02}{2} = 770.22At$$

$$F_{mC} = U_{mB} = \frac{Ni_B}{2} = \frac{22*-35.01}{2} = -385.11At$$

The negative value of currents of phases B and C must be applied to Fig. 1. and then the resulting configuration of currents in the slots of winding are (the A_0 represents returning wire of coil A):

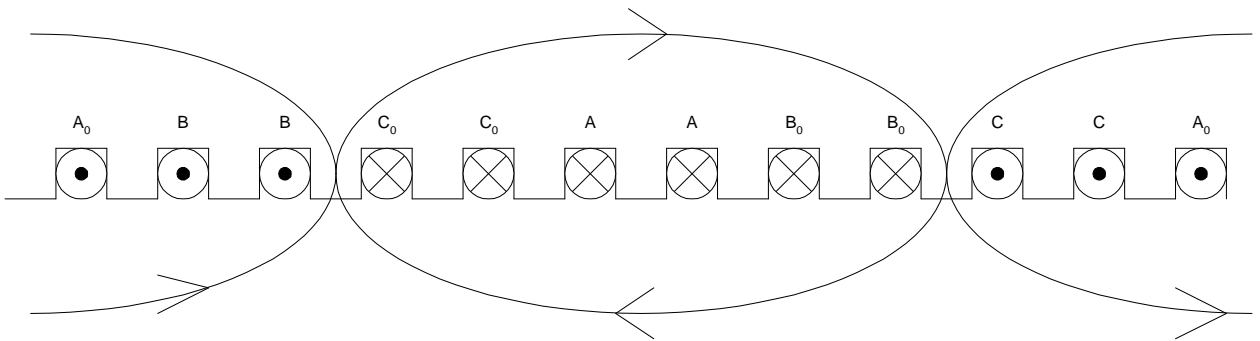


Fig. 12. Currents in the winding with their fluxpaths.

The polarity orientation of the voltage supplies in the model must be in the same direction as the fluxpaths in the Fig. 12..

3.2 Air gap components

Air gap in this machine is very specific because of the shape of the poles of rotor. So we need to simplify it by dividing it to a constant minimal air gap and two rectangles which dimension is average value of the selected range. Calculation of these average values is in chart 1..

$\theta [^{\circ}]$	g [mm]	avg [mm]
0	1,15	
1	1,15	
2	1,16	
3	1,18	
4	1,20	
5	1,22	
6	1,26	
7	1,30	
8	1,36	1,22
9	1,42	
10	1,50	
11	1,60	
12	1,72	
13	1,87	
14	2,06	
15	2,30	
16	2,62	2,33
17	3,07	
18	3,72	
22,5	6,44	4,41

Table 1. Calculation of average airgap on selected ranges.

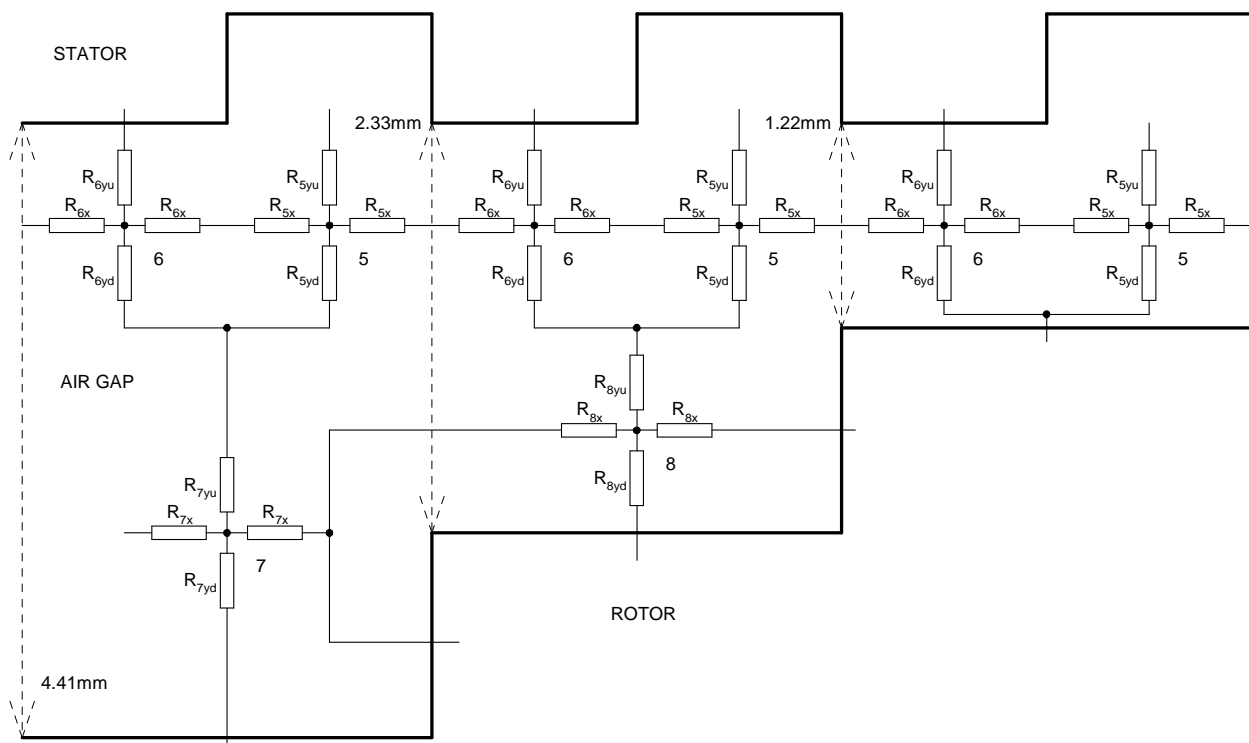


Fig. 13. Electric network representing magnetic reluctances of air gap.

Calculation of air gap resistors:

As mentioned before all sizes of segments were obtained from the blueprint of machine in Autodesk Inventor.

$$S_{5x} = 1.22 * 200 = 244 \text{ mm}^2$$



$$l_{5x} = 2.404/2 = 1.202 \text{ mm}$$

$$R_{5x} = \frac{1.202 \cdot 10^{-3}}{\mu_0 \cdot 244 \cdot 10^{-6}} = 3920.2 \text{ kH}^{-1}$$

$$S_{5yu} = 2.413 \cdot 200 = 482.6 \text{ mm}^2$$

$$l_{5y} = 1.22/2 = 0.61 \text{ mm}$$

$$R_{5yu} = 1005.8 \text{ kH}^{-1}$$

$$S_{5yd} = 2.395 \cdot 200 = 479 \text{ mm}^2$$

$$R_{5yd} = 1013.4 \text{ kH}^{-1}$$

$$S_{6x} = 1.22 \cdot 200 = 244 \text{ mm}^2$$

$$l_{5x} = 9.615/2 = 4.8 \text{ mm}$$

$$R_{6x} = 15654.6 \text{ kH}^{-1}$$

$$S_{6yu} = 9.651 \cdot 200 = 1930.2 \text{ mm}^2$$

$$l_{6y} = 1.22/2 = 0.61 \text{ mm}$$

$$R_{6yu} = 251.5 \text{ kH}^{-1}$$

$$S_{6yd} = 9.579 \cdot 200 = 1915.8 \text{ mm}^2$$

$$R_{6yd} = 253.4 \text{ kH}^{-1}$$

$$S_{7x} = 3.19 \cdot 200 = 638 \text{ mm}^2$$

$$l_{7x} = 11.759/2 = 5.88 \text{ mm}$$

$$R_{7x} = 7333.5 \text{ kH}^{-1}$$

$$S_{7yu} = 11.86 \cdot 200 = 2372 \text{ mm}^2$$

$$l_{7y} = 3.19/2 = 1.595 \text{ mm}$$

$$R_{7yu} = 535 \text{ kH}^{-1}$$

$$S_{7yd} = 11.66 \cdot 200 = 2331.9 \text{ mm}^2$$

$$R_{7yd} = 544.3 \text{ kH}^{-1}$$

$$S_{8x} = 1.11 \cdot 200 = 222 \text{ mm}^2$$

$$l_{8x} = 11.895/2 = 5.95 \text{ mm}$$

$$R_{8x} = 21328.2 \text{ kH}^{-1}$$

$$S_{8yu} = 11.927 \cdot 200 = 2385.3 \text{ mm}^2$$

$$l_{8y} = 1.11/2 = 0.555 \text{ mm}$$

$$R_{8yu} = 185.2 \text{ kH}^{-1}$$

$$S_{8yd} = 11.863 \cdot 200 = 2372.7 \text{ mm}^2$$

$$R_{8yd} = 186.1 \text{ kH}^{-1}$$

3.3 Rotor components

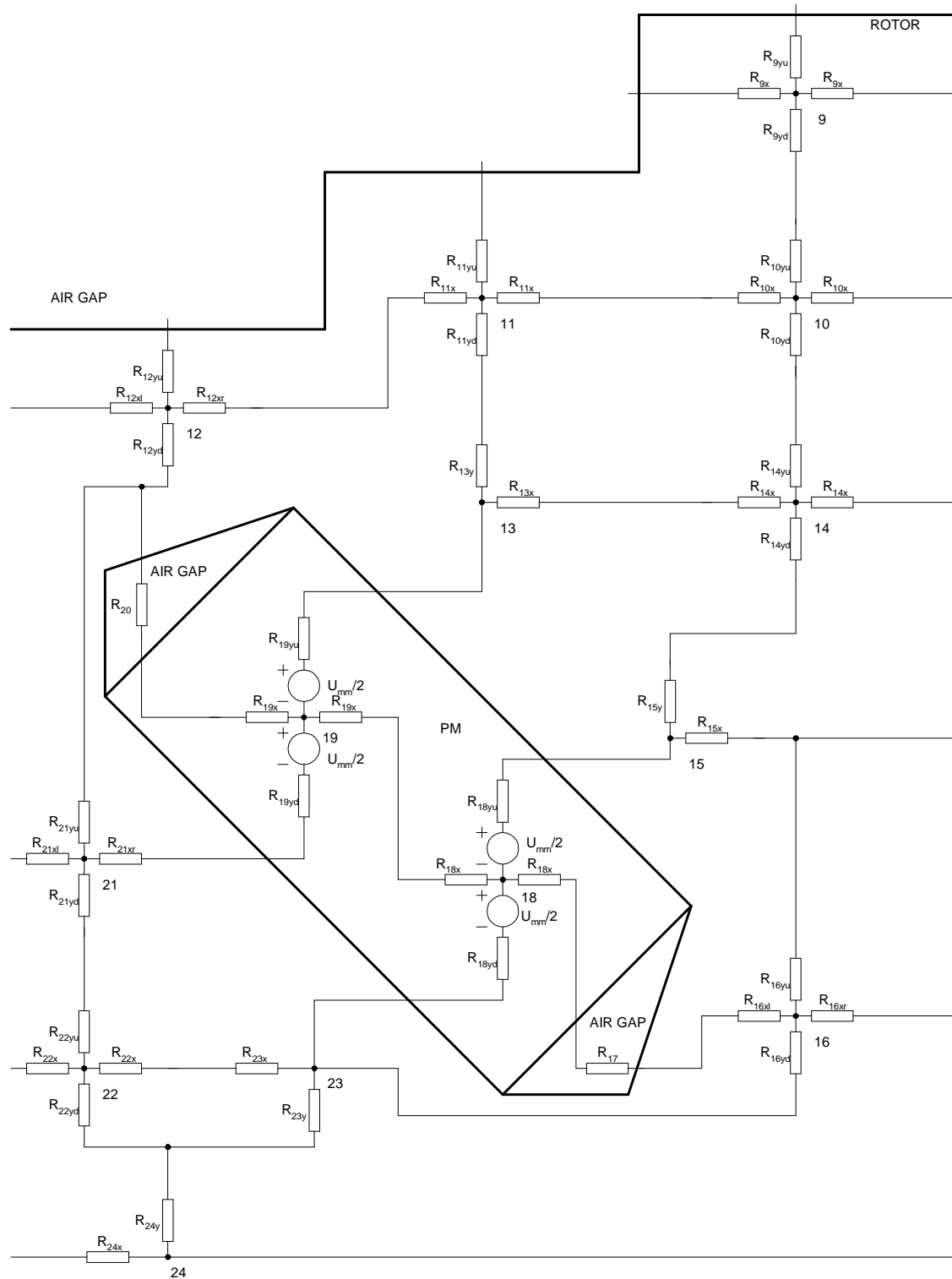


Fig. 14. Electric network representing magnetic reluctances of rotor.



$$R_{21xl}=207.4 \text{ H}^{-1}$$

$$R_{22yd}=837.8 \text{ H}^{-1}$$

$$R_{21yu}=2334.6 \text{ H}^{-1}$$

$$R_{23x}=1241.5 \text{ H}^{-1}$$

$$R_{21yd}=1130.4 \text{ H}^{-1}$$

$$R_{23y}=731.5 \text{ H}^{-1}$$

$$R_{22x}=1225.5 \text{ H}^{-1}$$

$$R_{24x}=382 \text{ H}^{-1}$$

$$R_{22yu}=779 \text{ H}^{-1}$$

$$R_{24y}=2535.9 \text{ H}^{-1}$$

Calculation of magnetic voltage generated by PM:

Parameters of PM are from datasheet that is in the enclosure of this work. The magnetic voltage is calculated with equation 2.9.

$$B_r=1.235 \text{ T}$$

$$\mu_r=1.05$$

$$l=10 \text{ mm}$$

$$F_{mm} = \frac{B_r l}{\mu_0 \mu_r} = \frac{1.235 * 0.01}{\mu_0 * 1.05} = 9359.8 At$$

4 PSPICE SIMULATION RESULTS

4.1 Model without winding current

Firstly we have made simulation of the model without winding current to see how it behaves. To simulate this machine we dont need to make model of entire machine but only a quarter of it and then connect the intersection with wires to the other side of it to encircle the fluxpaths. The complete electric network is too big to visualize it in the work so we will place only a sections of it. The whole network is in the enclosure of this work. The PSpice is software for simulating electrical circuits but we are using magnetoelectric equivalency so the current in simulation is representing magnetic flux. According to this if need to know magnetic flux density we use this equation:

$$B = \frac{\phi}{s} \quad (4.1)$$

Φ – magnetic flux (current in the simulation through a segment)

S – area of the segment which density we need to know

In one of the first simulations we were observing that only a fraction of magnetic flux is passing thru the airgap of the machine. After carefull review we realized that segments 12 and 16 acts as a magnetic short circuit and they are drawing nearly all of the magnetic flux supplied by PMs. These segments were oversaturated and it was happening because of their linear magnetic resistivity. To eliminate this error without making them nonlinear we raised the magnetic resistivity by multiplying it by 1000 to reach resistivity simmilar to air. By this step we eliminated these short circuits and the air gap magnetic flux raised to expected values.

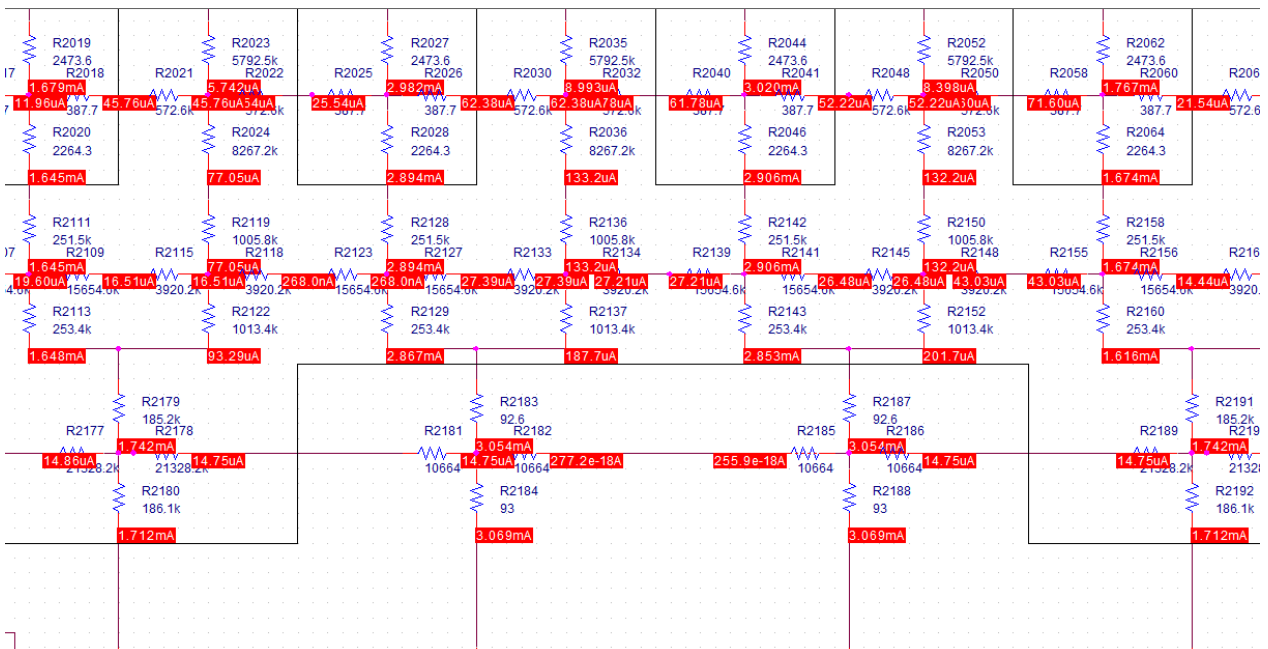


Fig. 16. Section of network representing air gap over the pole without winding.

The example of the section of network with corresponding currents representing magnetic fluxes is shown on Fig. 16.(the indexes of resistors are automatically generated by PSpice).

The distribution of magnetic flux over air gap is visualized in Fig. 17. in mechanical degrees.

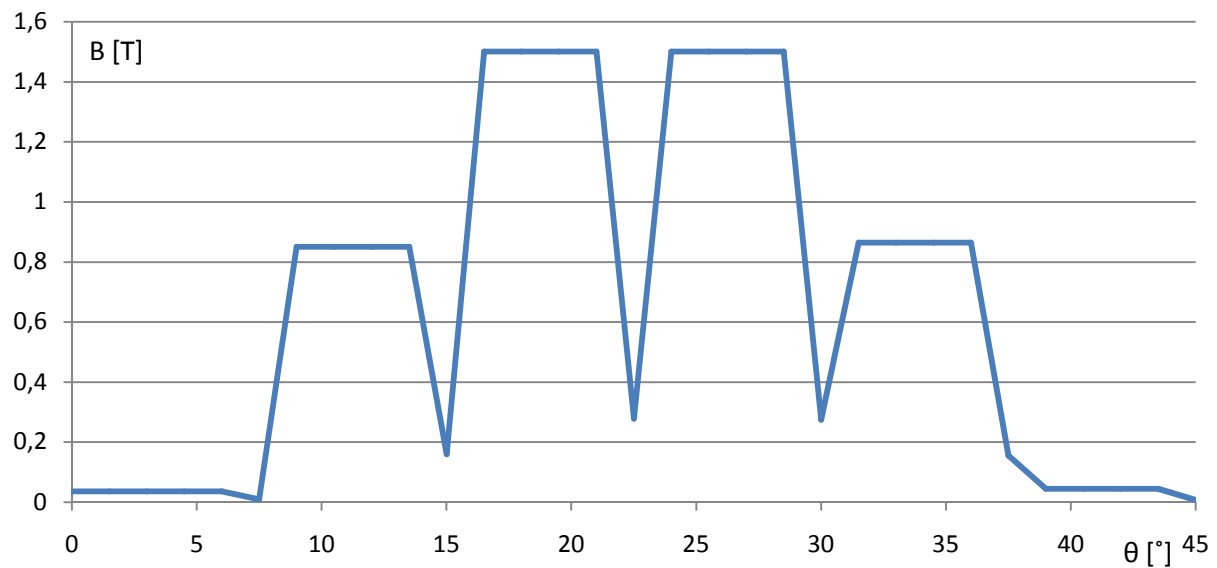


Fig. 17. Distribution of magnetic flux density over air gap without winding.

In graph on Fig. 17. we can see very good the influence of stator slots to the shape of the magnetic flux density of the machine. We also must mention that the value of density is greater than in the real machine and this is caused by the linear resistors representing the magnetic resistivity of steel which is nonlinear.

4.2 Model with winding current

After familiarizing with the simulation without winding we proceed to the complete static simulation. We placed voltage supplies representing winding to the corresponding segments over the slots and we oriented them correctly according to the Fig. 12.. The result of the part of simulation is on picture 18.. The whole network with simulation results is in enclosure.

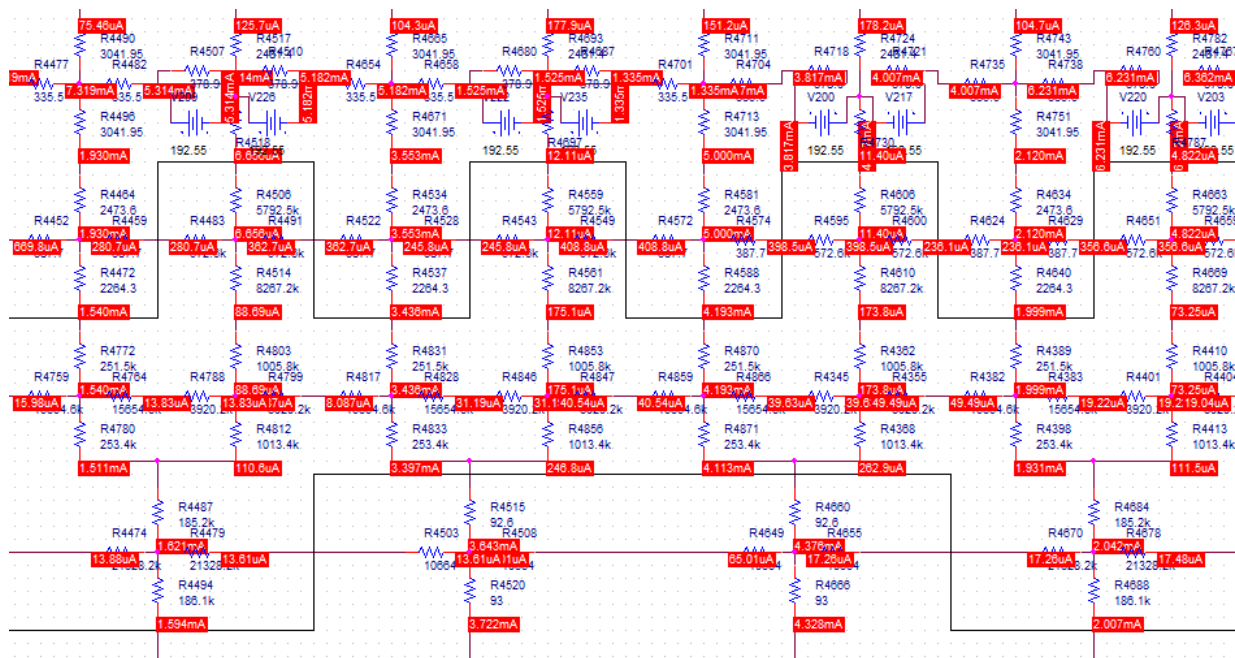


Fig. 18. Section of network representing air gap over the pole with winding.

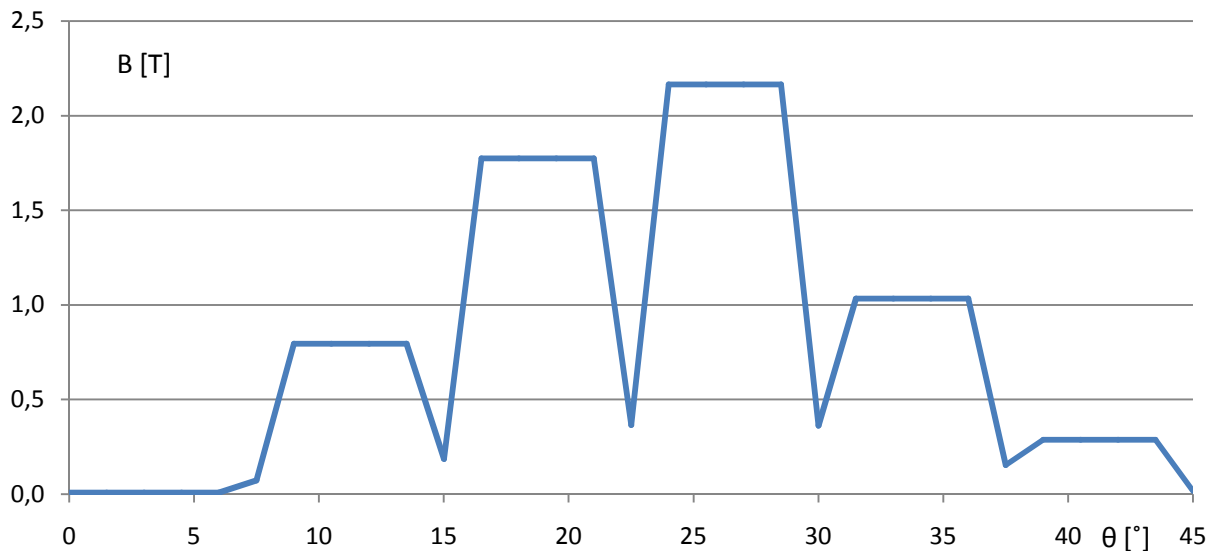


Fig. 19. Distribution of magnetic flux density over air gap with winding.

In graph on Fig. 19. we see a shift to the right side. This is caused by the placing of the rotor teeth which represents the magnetic pole of stator on the right side instead of center of the rotor pole. So this distribution corresponds to the situation when there is an angle between the stator and rotor resulting magnetic flux.

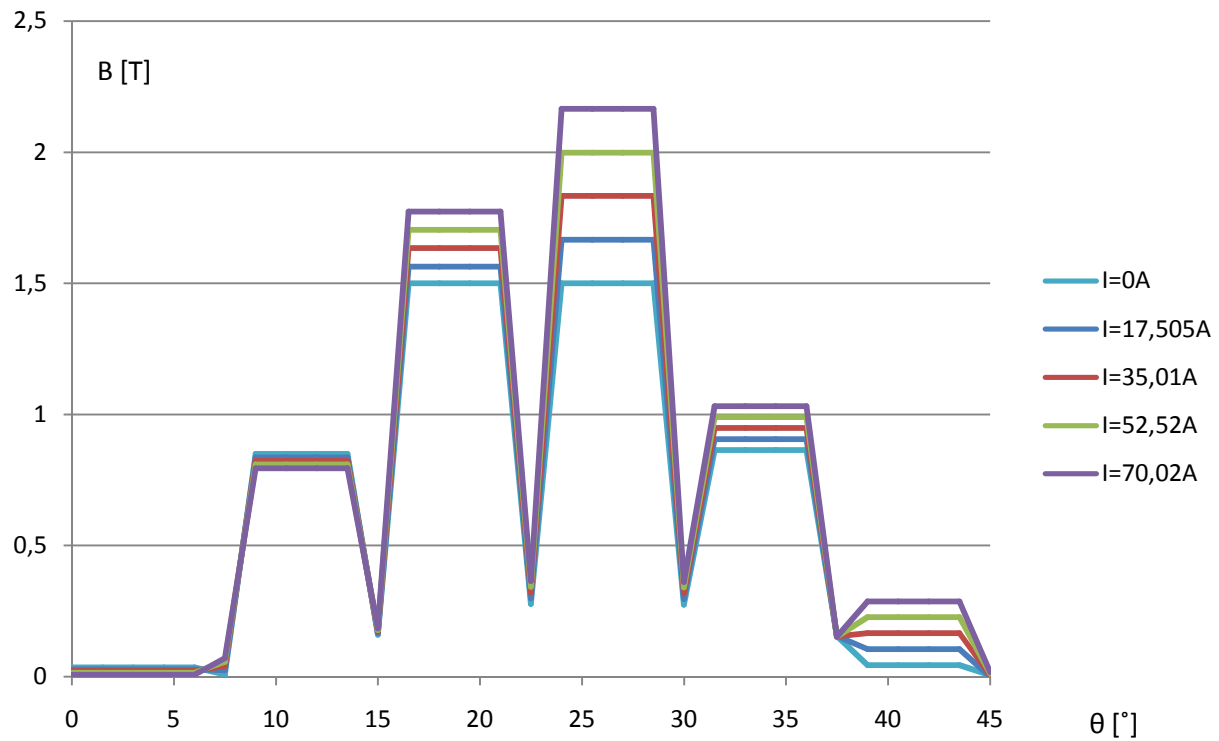


Fig. 20. Distribution of magnetic flux density over air gap with changing current.

We have also simulated models with lower currents. In the graph on Fig. 20. we can see the change of magnetic flux density with increasing current thru the coil of winding. The corresponding chart and simulations are in the enclosure of this work. The nominal value of current in coil A is 50,92Arms (70,02Apeak) and in the graph we have visualized results of simulations with currents below this value also including zero value which is same as graph on Fig. 17.. We can see that the change of density is same with each step of increase of the current so it is linear function. This is caused by using linear magnetic resistors and with using the nonlinear resistors also this function will be nonlinear.

On the other hand the value above 2 T is too high for this machine and we think it is also caused by the linear resistors representing the magnetic resistivity of steel which is nonlinear. Also some segments in this simulation are oversaturated. We think that these problems will be solved by placing nonlinear resistors to the network and then the results will match very accurately with real values of these parameters.

5 IMPROVING OF PSPICE MODEL

5.1 Nonlinear resistors

As we mentioned before the results of magnetic flux densities in simulations were too high because of the linear resistors representing steel sheets. So we must replace them with nonlinear resistors corresponding to the BH curve of the used material. In the PSpice software there is not such component. So after some search we realized that we can use GVALUE part, which is voltage input dependent current source that can be programmed with mathematical equations. We used following connection of GVALUE part (Fig. 21.).

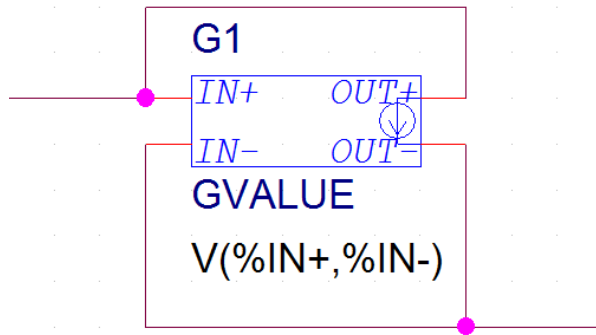


Fig. 21. GVALUE part connection.

The current output of this part is defined by equation:

$$I = G \cdot U \quad (4.1)$$

The voltage U is represented with $V(\%IN+, \%IN-)$ inscription. We need to input BH curve data to the equation which will make the resistor behave nonlinearity. To do this we use TABLE command which is linear approximation function. Input to this function must be H and it will give us back B on the part which is resistor representing corresponding to the BH curve. After that we must recalculate it to the magnetic flux using length l and area S of the segment which is represented by this resistor. We use following equations ($F_m = U$, $\Phi = I$):

$$H = \frac{F_m}{l} \quad (4.2)$$

$$\phi = B \cdot S \quad (4.3)$$

For the segment that $l=4,247\text{mm}$ and $S=4460\text{mm}^2$ which are R_{1x} resistor parameters the final inscription will be:

TABLE((1/0.004247)*V(%IN+,%IN-),+ -30000,-2,-7000,-1.7,-1800,-1.5,-170,-1.2,0,0,170,1.2,1800,1.5,7000,1.7,30000,2)*(0.00446)

The length of the inscription of GVALUE part is limited so we can not put the whole BH curve data but only the main points of the curve (Fig. 22.). Also we must define the negative values to have this resistor symmetrical in positive and negative voltage.

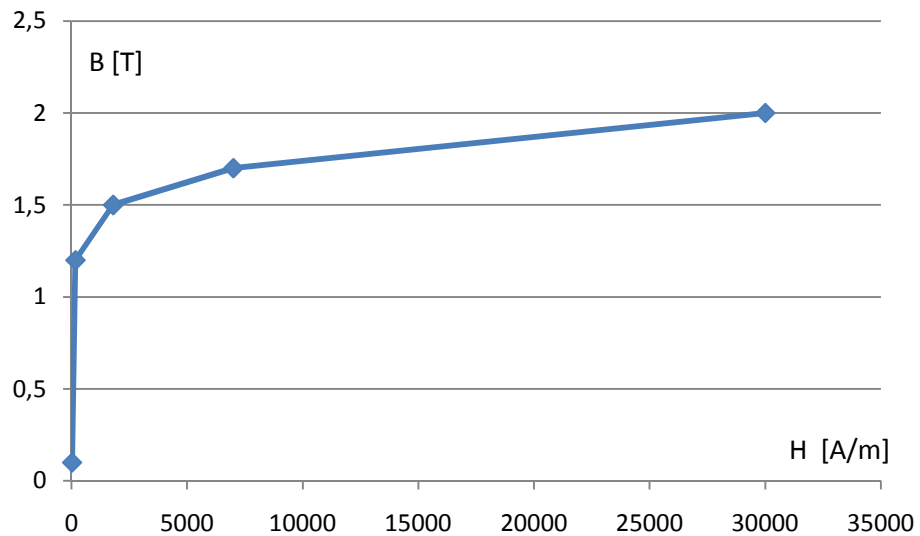


Fig. 22. BH curve of the M235-35A steel inscribed to GVALUE part.

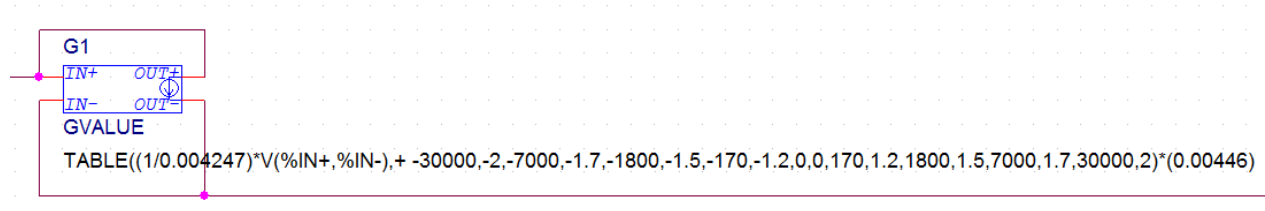


Fig. 23. GVALUE part representing R_{Ix} .

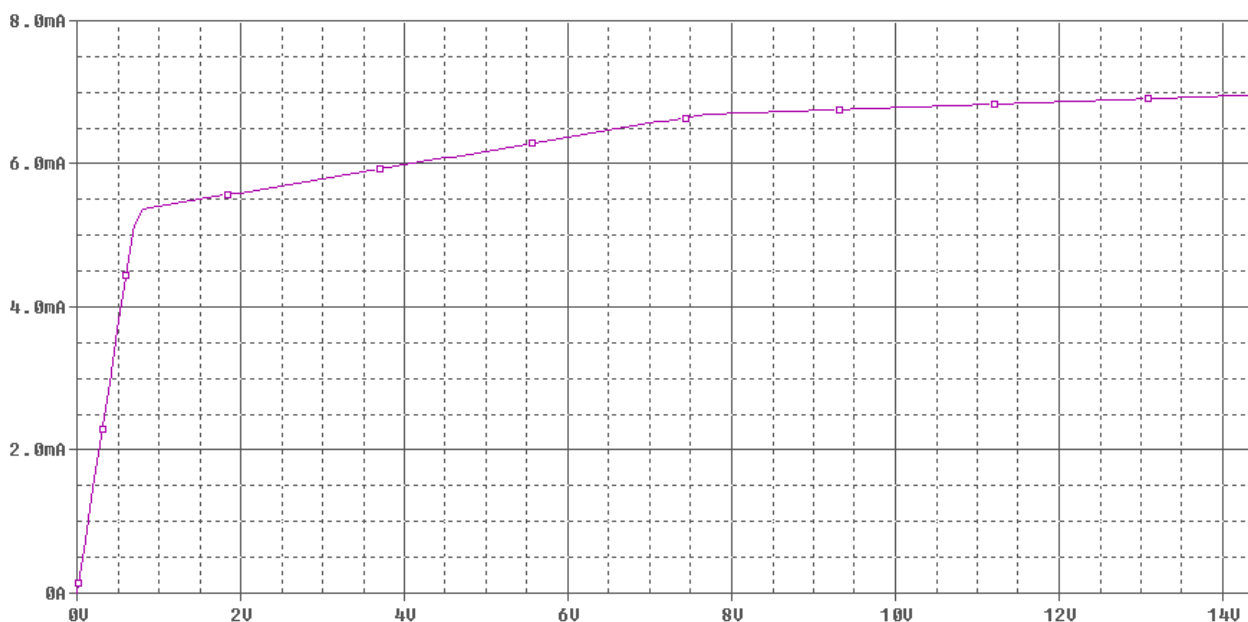


Fig. 24. Nonlinear behavior of GVALUE part representing R_{Ix} .

Then we replaced every resistor in the simulation representing steel sheets with GVALUE parts with corresponding values of length and area (Fig.25.). And we visualized the value of magnetic

flux density over air gap over a pole of machine without and with nominal current in the winding (Fig.26.). Also the problem with magnetic short circuit on rotor segments 12 and 16 was solved.

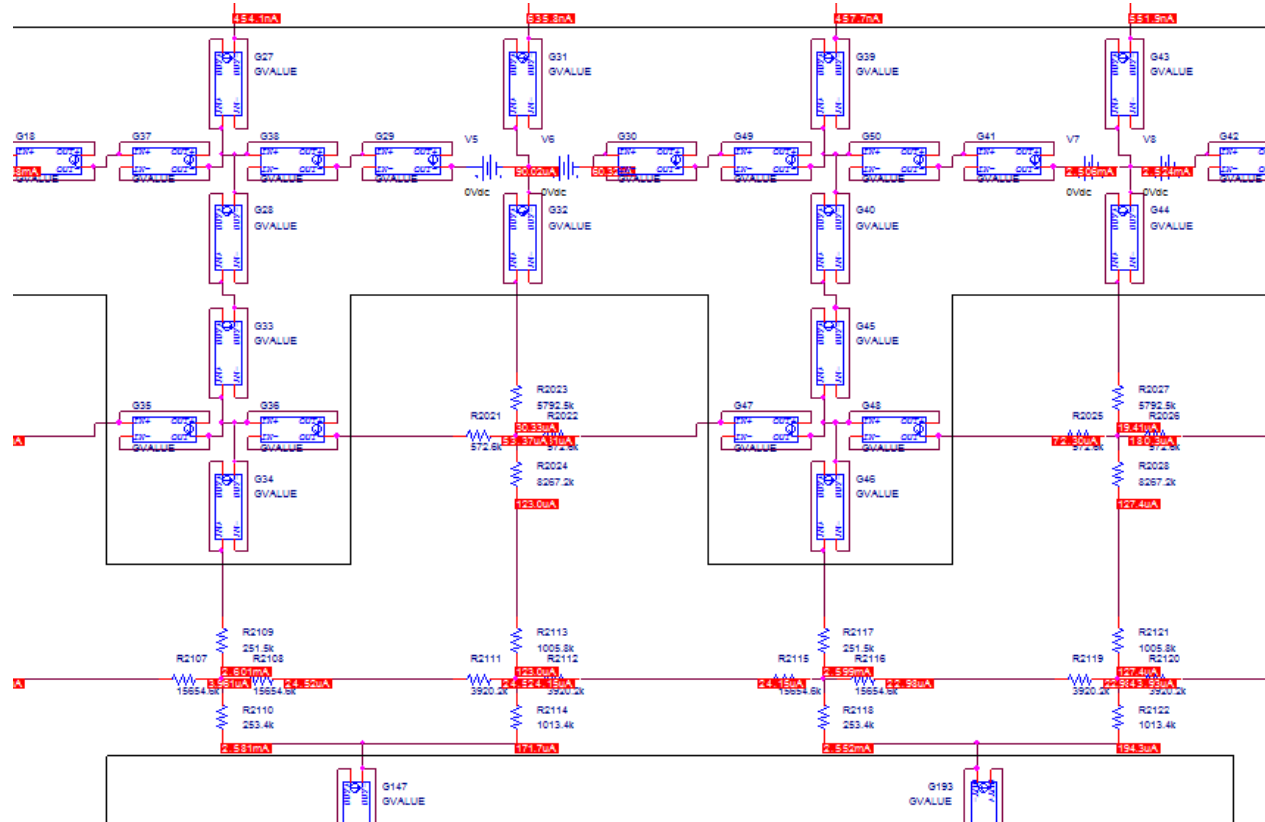


Fig. 25. Section of network over pole with nonlinear resistors.

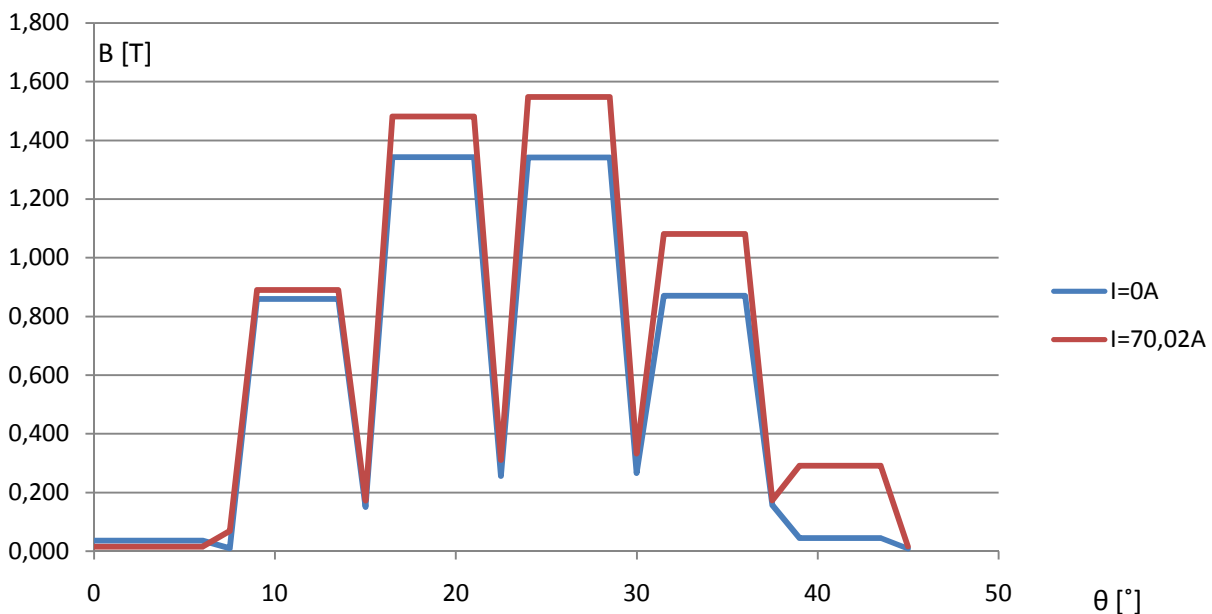


Fig. 26. Magnetic flux density over air gap with nonlinear resistors with zero and nominal current in winding.



5.2 Working temperature of PM

In our model we calculated with magnetic flux density of permanent magnets at 20°C but we must take into consideration that working temperature of PM in this machine is 70°C and this will decrease the magnetic flux density of magnet and also in the air gap. Parameters of N38EH magnet:

B_{r20}= 1,24T (Coercive force at 20°C)

μ_r= 1,08 (Recoil permability)

α_B= -0,11 (Temperature coefficient of B)

T= 70°C (Working temperature)

$$B_{rT} = B_{r20} \left(1 + \frac{\alpha_B}{100} (T - 20) \right) = 1,24T \left(1 + \frac{-0,11}{100} (70 - 20) \right) = 1,1718T \quad (4.4)$$

According to this magnetic flux density we must recalculate the magnetic voltage of the PM in the rotor of the machine and change that value in the model. This will decrease the air gap flux density to real value.

$$F_{mm} = \frac{B_r l}{\mu_0 \mu_r} = \frac{1.1718 * 0.01}{\mu_0 * 1.08} = 9099,83At$$

5.3 Angle shift of rotor

To achieve angle shift of the rotor we again used GVALUE part, but with different equations. We realized that during angle shift between -90° to +90° electrical each segment of rotor is connected maximally to 6 nearest teeth segments through the air gap. The selection of the concrete segment depends of exact value of the angle shift. Also to simplify this switching we replaced the segments 5 and 6 of air gap with one segment.

$$S_{5x}=244mm^2$$

$$l_{5x}=2,404mm$$

$$l_{6x}=9,615mm$$

$$l_{56x}=12,019/2=6$$

$$R_{56x} = \frac{6*10^{-3}}{\mu_0 * 244 * 10^{-6}} = 19568,23kH^{-1}$$

$$l_{56x}=0,61mm$$

$$S_{56yu}=482,6+1930,2= 2412,8mm^2$$

$$R_{56yd} = \frac{0,61 * 10^{-3}}{\mu_0 * 2412,8 * 10^{-6}} = 201,19kH^{-1}$$

$$S_{56yd}=479+1915,8= 2394,8mm^2$$



$$R_{56yd} = \frac{0,61 \cdot 10^{-3}}{\mu_0 \cdot 2394,8 \cdot 10^{-6}} = 202,7 \text{ kH}^{-1} \Rightarrow G_{56yd} = \frac{1}{202,7 \text{ kH}^{-1}} = 4,933 \mu\text{H}$$

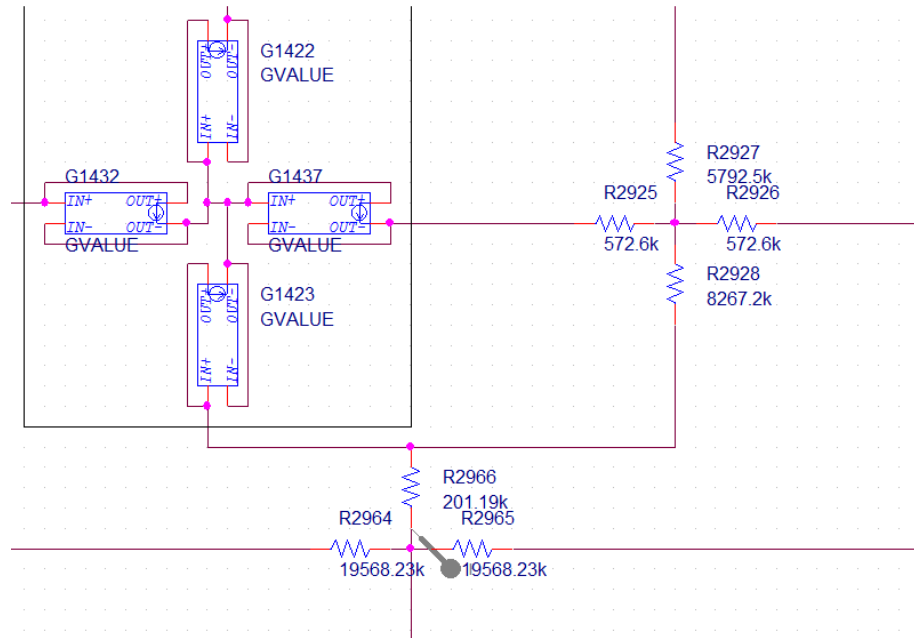


Fig. 27. Part of network with replaced air gap segments.

We can see in Fig.26. how we replaced the segment 5 and 6 with one segment. Also we can see that on this figure is missing the R_{56yd} resistor. That is because we will replace him with GVALUE part which will have conductivity G_{56yd} in the fully switched state.

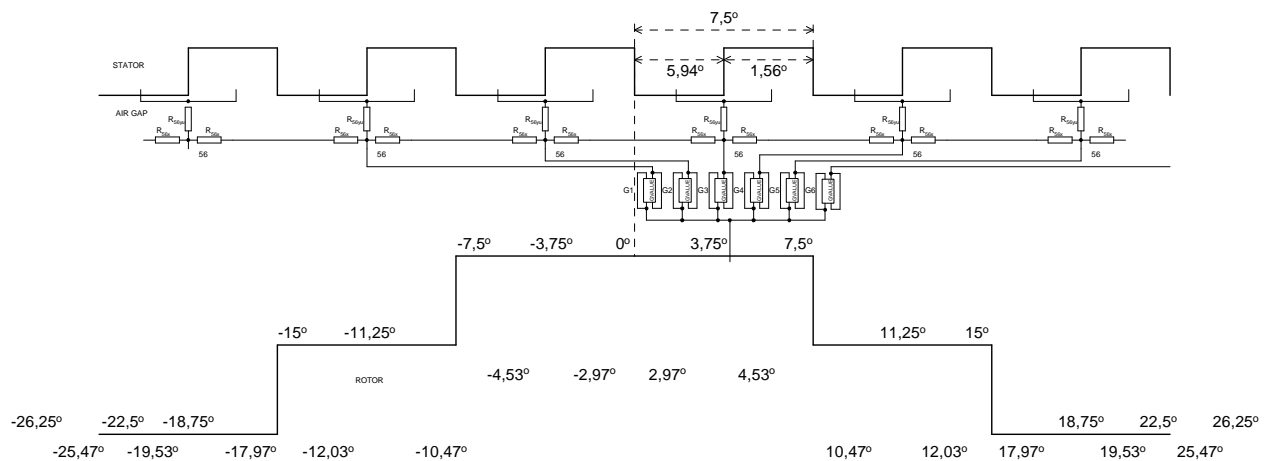


Fig. 28. One rotor segment connection.

On Fig.28. we can see the right rotor segment connected to 6 nearest teeth through airgap resistors R_{56yd} represented with GVALUE part. All angles on the figure are mechanical. The angles at bottom are overlapping angles in which the according teeth is conductively connected to the rotor segment. The angle is calculated as 0 plus half of the teeth angle and 7,5 minus half of the teeth angle for rotor segment connected on the Fig.28. and for the next segments it is calculated similary.

The GVALUE parts are enscripted:

- G1: V(%IN+,%IN-)*TABLE(A,12.03,1p,17.97,4.93u,19.53,4.93u,25.47,1p)
 G2: V(%IN+,%IN-)*TABLE(A,4.53,1p,10.47,4.93u,12.03,4.93u,17.97,1p)
 G3: V(%IN+,%IN-)*TABLE(A,-2.97,1p,2.97,4.93u,4.53,4.93u,10.47,1p)
 G4: V(%IN+,%IN-)*TABLE(A,-10.47,1p,-4.53,4.93u,-2.97,4.93u,2.97,1p)
 G5: V(%IN+,%IN-)*TABLE(A,-17.97,1p,-12.03,4.93u,-10.47,4.93u,-4.53,1p)
 G6: V(%IN+,%IN-)*TABLE(A,-25.47,1p,-19.53,4.93u,-17.97,4.93u,-12.03,1p)

The A parameter in the inscription is shift of the rotor in mechanical angles which is declared in PSpice include file .inc as follows .PARAM A value. This is input angle which defines angle shift of rotor in mechanical degrees (at zero teeth is at the center of the rotor pole). From the G3 part inscription we can see that the teeth above the rotor segment is connected to it from angle $2,97^\circ$ to $4,53^\circ$ with conductivity $G_{56yd} = 4,933\mu\text{H}$ and then to the nearest overpassing angles $-2,97^\circ$ and $10,47^\circ$ the conductivity is decreasing linearly. For better understanding we can see this in parametric simulation with changing angle from $-22,5^\circ$ to $22,5^\circ$ on Fig.29.(the currents are just demonstrative).

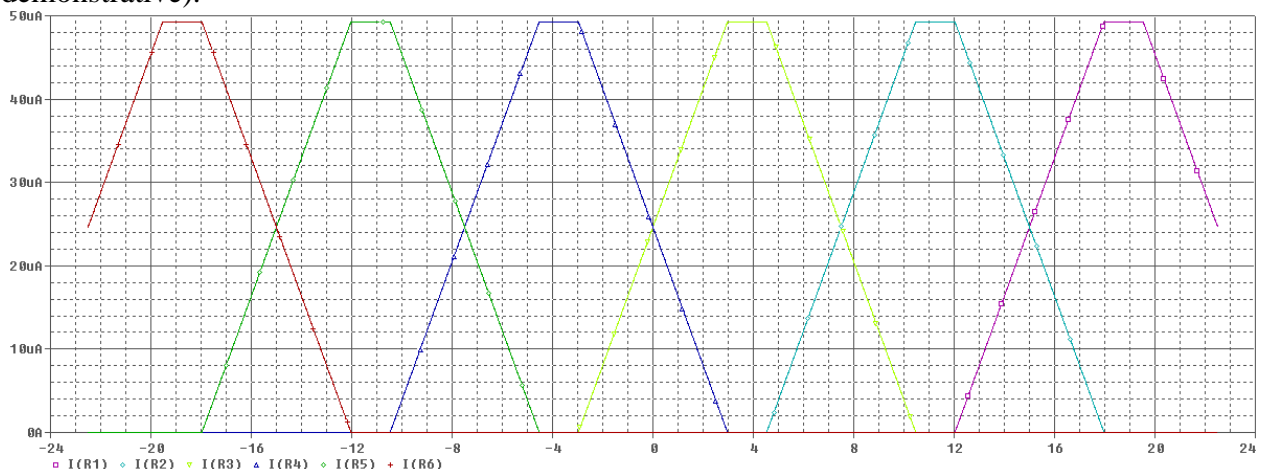


Fig. 29. Changing of conductivity with angle.

We connected all rotor segments to according teeth with this technique and we get a model in which we can by defining the parameter A change the angle shift of rotor.

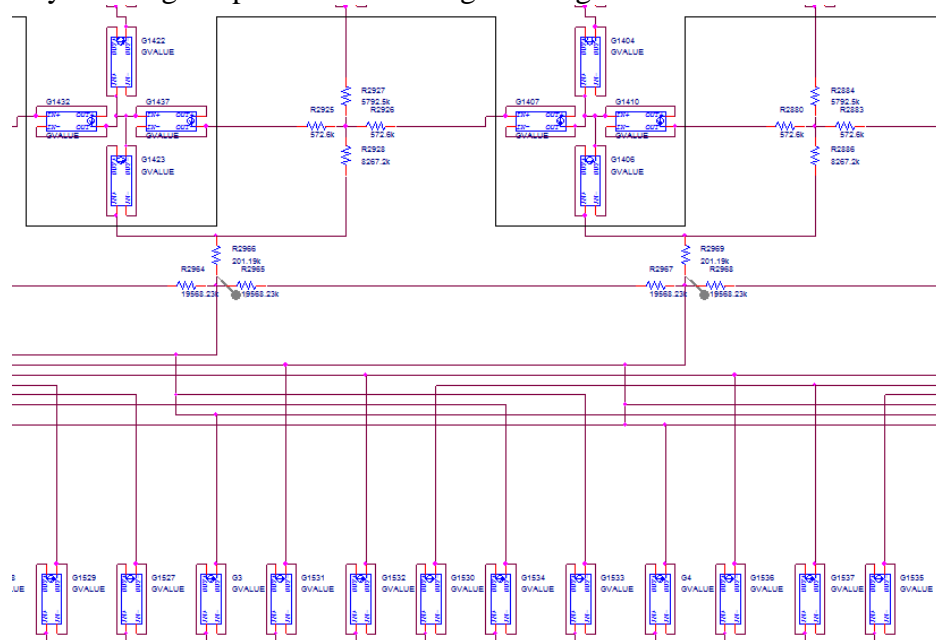


Fig. 30. Part of the network with angle shift.



Later in this work we calculate induced voltage u_i at the nominal rpm. The voltage is calculated as a derivation of average magnetic flux through one coil in time. We would discuss this problem more in next chapter but in short – linear change of fair gap conductivity and also its constant value makes the derivation with peaks and too many zero values of u_i . The conductivity and also magnetic flux through the air gap changes continuously in the real machine. So we must change the shape of the changing conductivity. We realized that we can change the trapezium shape to cosinus function with equivalent area. After some calculation and testing we get these equations of cosinus function for G3 part:

$$-2,465\mu \cdot \cos(2\pi \cdot 0,66667 + 0,25 \cdot 2\pi) + 2,465\mu$$

The GVALUE parts with cosines function are enscripted:

G1: $V(\%IN+, \%IN-)*(-2.465u*\cos(2*PI*0.0666667*A - 0.75*2*PI) + 2.465u)*TABLE(A, 11.24, 1p, 11.25, 1, 26.25, 1, 26.26, 1p)$
G2: $V(\%IN+, \%IN-)*(-2.465u*\cos(2*PI*0.0666667*A - 0.25*2*PI) + 2.465u)*TABLE(A, 3.74, 1p, 3.75, 1, 18.75, 1, 18.76, 1p)$
G3: $V(\%IN+, \%IN-)*(-2.465u*\cos(2*PI*0.0666667*A + 0.25*2*PI) + 2.465u)*TABLE(A, -3.76, 1p, -3.75, 1, 11.25, 1, 11.26, 1p)$
G4: $V(\%IN+, \%IN-)*(-2.465u*\cos(2*PI*0.0666667*A + 0.75*2*PI) + 2.465u)*TABLE(A, -11.26, 1p, -11.25, 1, 3.75, 1, 3.76, 1p)$
G5: $V(\%IN+, \%IN-)*(-2.465u*\cos(2*PI*0.0666667*A + 1.25*2*PI) + 2.465u)*TABLE(A, -18.76, 1p, -18.75, 1, -3.75, 1, -3.74, 1p)$
G6: $V(\%IN+, \%IN-)*(-2.465u*\cos(2*PI*0.0666667*A + 1.75*2*PI) + 2.465u)*TABLE(A, -26.26, 1p, -26.25, 1, -11.25, 1, -11.24, 1p)$

For better understanding we can see the comparison of the trapezium and cosinus shaped conductivity changes in Fig.31..

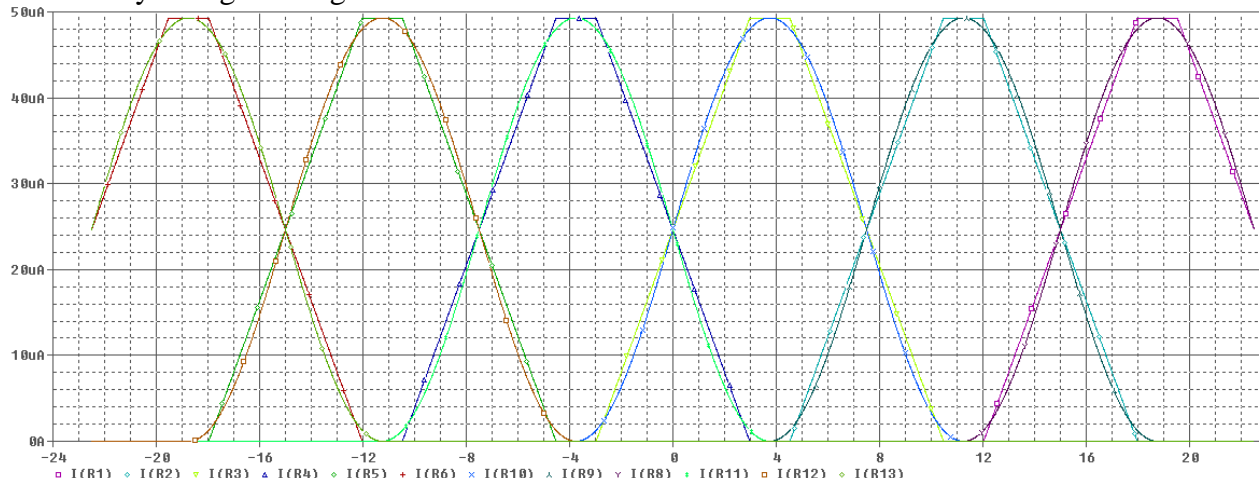


Fig. 31. Comparison of trapezium and cosinus change of conductivity.

We also calculate the G3 part conductivity area of this functions to be sure we have equal areas.
Trapezium:

$$S = 4,933\mu \cdot (4,53 - 2,97) + 4,933\mu \cdot (10,47 - 4,53) = 36,975\mu$$

Sinus:

$$S = \int_{-3,75}^{11,25} -2,465\mu \cdot \cos(2\pi \cdot 0,66667 + 0,25 \cdot 2\pi) + 2,465\mu = 36,9748\mu$$

With using cosinus shaped change of conductivity we get better shape of induced voltage u_i .

6 FINAL PSPICE SIMULATION RESULTS

6.1 No load test

To compare our results with my colleague Bc. Petr Chmelíček, who is making the model of the same machine with FEM method using Ansys software [2], we calculated distribution of magnetic flux density in the air gap during no load test at 0° angle shift of rotor with zero current in the winding.

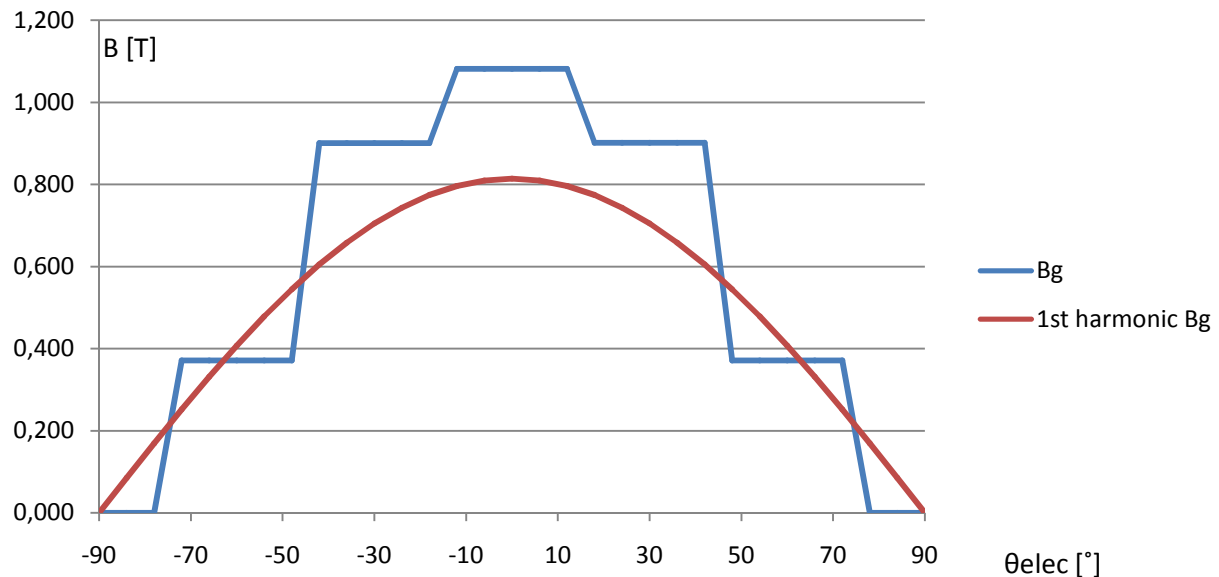


Fig. 32. Distribution of magnetic flux density in the air gap during no load test (PSpice model).

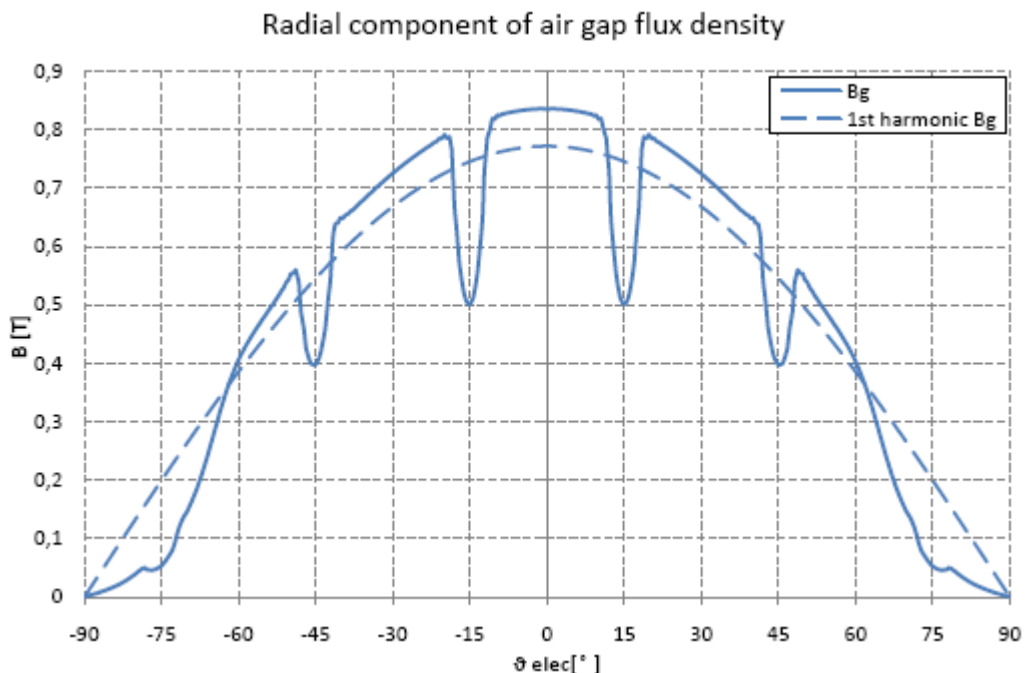


Fig. 33. Distribution of magnetic flux density in the air gap during no load test (FEM calculation) [2].



The B_g in our graph (Fig.32.) was calculated as a magnetic flux through the segment divided by its area:

$$B_g = \frac{\phi}{S} = \frac{2,598 \cdot 10^{-3} Wb}{2403 \cdot 10^{-6} m^2} = 1,081 T$$

The 1st harmonic was calculated as a sum of the flux densities through the pole divided by the area of pole multiplied with $\pi/2$ to get the amplitude:

$$B_{gAMP} = \frac{\sum_1^7 \phi \pi}{\sum_1^7 S \frac{\pi}{2}} = \frac{8,7113 \cdot 10^{-3} Wb}{16826,6 \cdot 10^{-6} mm^2} \frac{\pi}{2} = 0,8135 T$$

The FEM method calculated results can be seen in Fig.33. When we compare the figures 32. And 33. we can see that our PSpice calculated values of B_g are slightly higher but the 1st harmonic of B_g is very similar. The PSpice calculation is very fast (few seconds) but the results need to be interpreted correctly according to the construction of the machine (winding, pole areas,...) to get graphical charts that can be compared to Ansys FEM method calculated diagrams.

6.2 Induced voltage calculation

We made a parametric simulation with changing the rotor angle shift from $-22,5^\circ$ to $22,5^\circ$ with step $0,01^\circ$ and we visualized all 12 segments (2 poles) flux densities (Fig.34.).

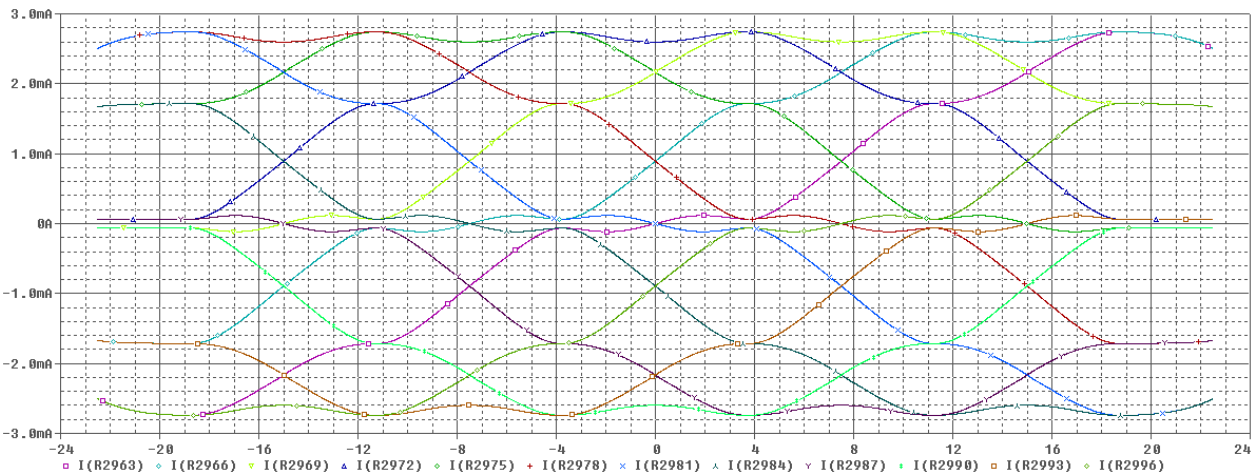


Fig. 34. Change of magnetic flux through segments according to angle shift ($I=\Phi$).

To calculate the induced voltage u_i we assume that rotor is rotating at the nominal speed 1300 rpm and the visualized voltage will be induced in one coil.

$$u_i = \frac{d\psi}{dt} = \frac{Nd\phi}{dt}$$

$$N=4.22=88$$

$$n=1300 \text{ rpm} \Rightarrow 21,667 \text{ s}^{-1} \Rightarrow 7800,12^\circ/\text{s}$$

$$360^\circ \Rightarrow 0,04615 \text{ s}$$

$$\text{one step}=0,01^\circ \Rightarrow dt=1,282 \cdot 10^{-6} \text{ s}$$

As magnetic flux through the coil we assume average value of the magnetic fluxes through the coil, corresponding to winding it is first 7 fluxes (Fig.35.).

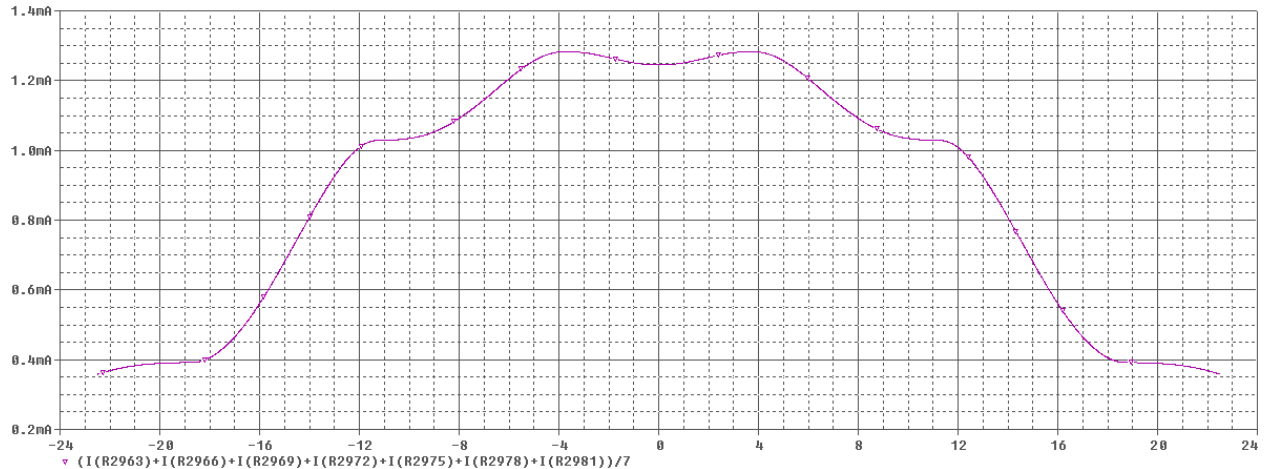


Fig. 35. Average value of magnetic flux through one coil ($I=\Phi$).

We exported the data from Fig.35. to Excel and according to u_i equation we execute numerical derivation to get the shape of u_i . The chart according to the step size has 4500 rows so it is not enclosed. Firstly we were using trapezium change of conductivity in the air gap which gave us unreal results of the shape of u_i (Fig.36.). After that we used cosinus change of conductivity in air gap which gave us better shape of u_i (Fig.37.).

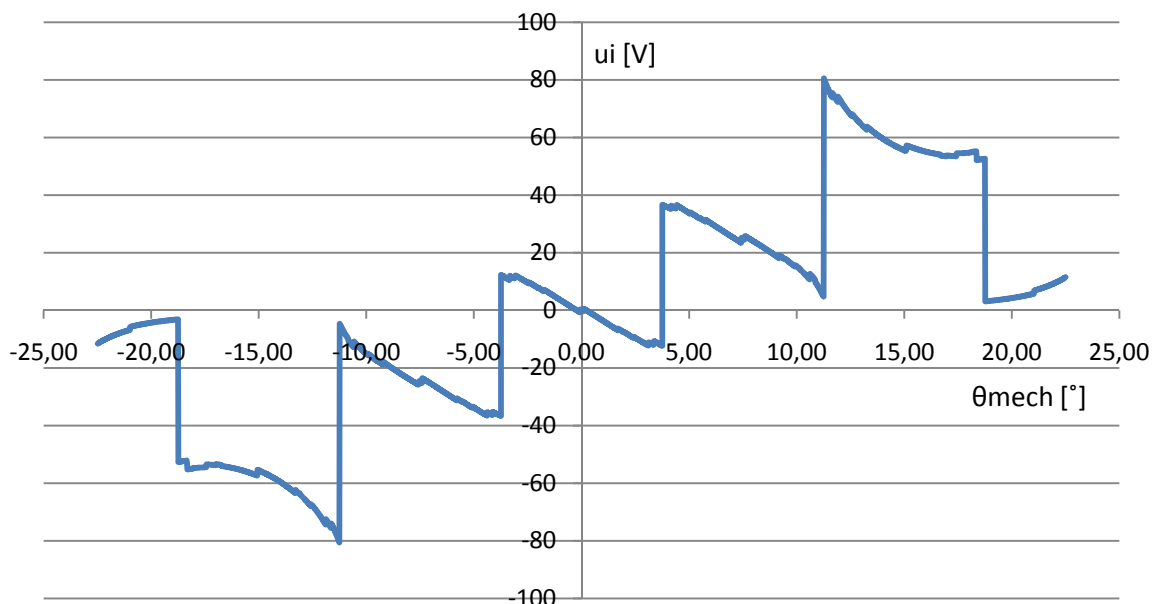


Fig. 36. Shape of the u_i with trapezium change of conductivity in air gap.

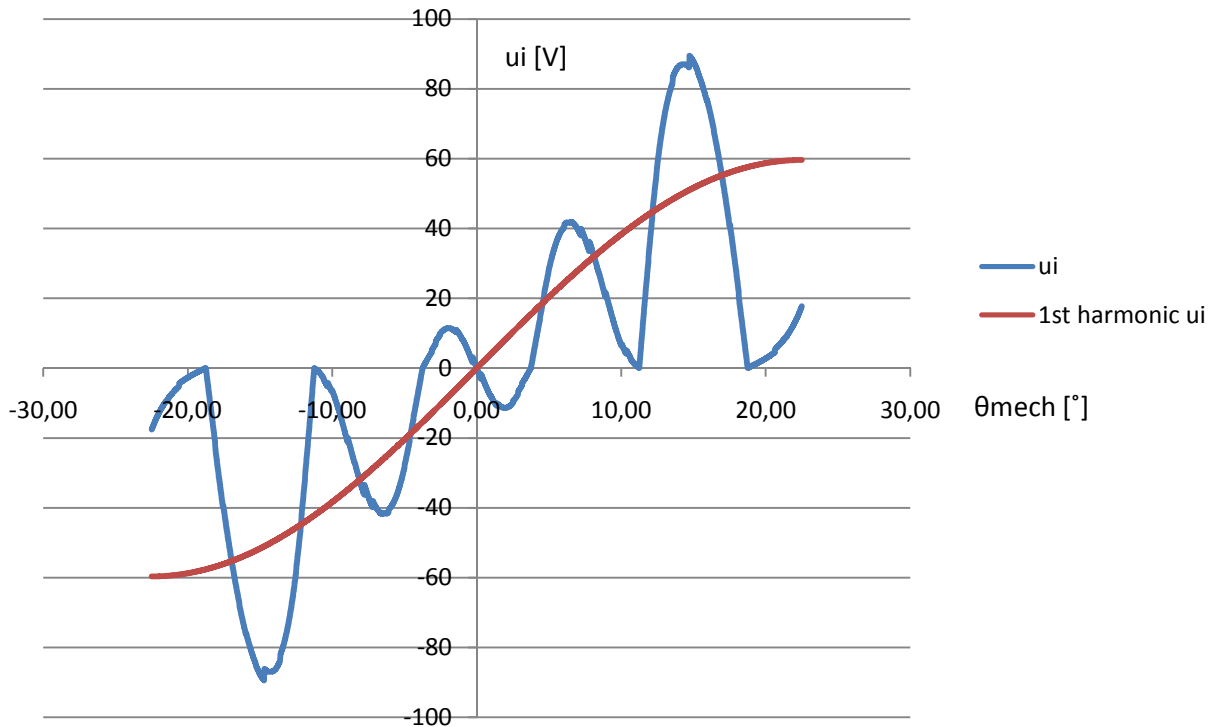


Fig. 37. Induced voltage u_i .

We make also numerical derivation of the 1st harmonic of B_g from the no load test (Fig. 32.) and we get the 1st harmonic of u_i that as we can see on figure 37. describes the same area as the u_i calculated directly from the segment fluxes. The value of the 1st harmonic of B_g was recalculated to middle value and then to average value of the magnetic flux through the one coil to get the correct result.

6.1 Power and torque calculation

We calculated power and torque of the machine from two different equations so we can be sure that the results are right if the two equations give same results. In both equations we used subsidiary circuits to calculate all needed parameters. We assumed that the machine is working as a generator at nominal rpm. Firstly we calculated according to this equation:

$$P = 3 \left(\frac{U_i \cdot U_1}{\omega_s \cdot L_d} \sin \beta + U_1^2 \frac{L_d - L_q}{2 \cdot \omega_s \cdot L_d \cdot L_q} \sin 2\beta \right) \quad (6.1)$$

We know these parameters:

$$L_d = 0,3268 \text{ mH}$$

$$L_q = 0,6089 \text{ mH}$$

$$f = 1300 \text{ rpm} / 60 = 21,667 \text{ Hz}$$

$$U_i = 59,65 \text{ V} / \sqrt{2} = 42,17 \text{ V}$$

Only one unknown parameter is voltage U_1 which we can get from subsidiary circuit of machine.

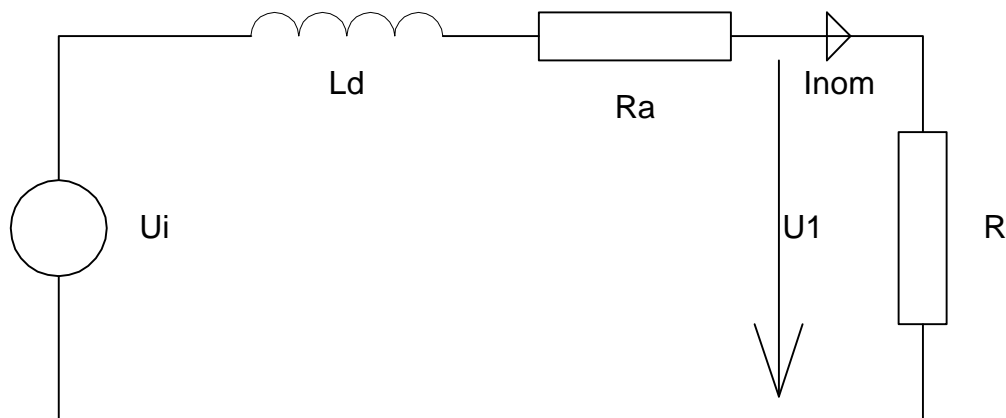


Fig. 38. Reciprocal circuit of machine.

In reciprocal circuit (Fig. 38.) the $R_a = 0,0281\Omega$ is phase resistance which we know from parameters of machine and the R is the load of the machine that the $I_{nom}=203,7A$.

$$I_{nom} = \frac{U_i}{Z} = \frac{U_i}{\omega \cdot L_d + R_a + R}$$

$$R = \frac{U_i}{I_{nom}} - \omega \cdot L_d - R_a = \frac{42,17}{203,7} - 2 \cdot \pi \cdot 21,667 \cdot 0,0003268 - 0,0281 = 0,1344\Omega$$

$$U_1 = R \cdot I_{nom} = 0,1344 \cdot 203,7 = 27,38V$$

When we have all needed parameters we calculated the power of the machine according to the change of load angle β .

$$P = 3 \left(\frac{27,38 \cdot 42,17}{2 \cdot \pi \cdot 21,667 \cdot 0,0003268} \sin \beta + 27,38^2 \frac{0,0003268 - 0,0006089}{2 \cdot 2 \cdot \pi \cdot 21,667 \cdot 0,0003268 \cdot 0,0006089} \sin 2\beta \right)$$

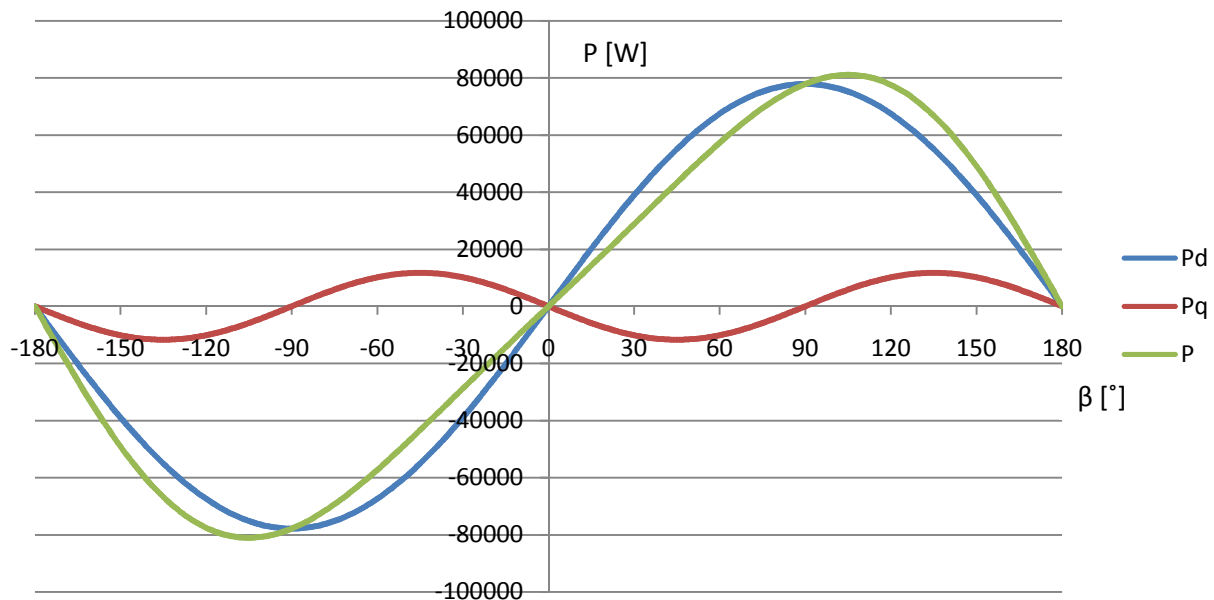


Fig. 39. Power characteristic of the synchronous machine according to load angle from first equation.

Nominal power of machine from first equation is:

$$P_{nom} = \frac{\int_{0^\circ}^{180^\circ} P d\beta}{180} = 49564W$$

We also calculated the power and torque of machine from this equation to verify our results:

$$P = 3 \cdot M \cdot \omega = 1,5 \cdot pp (\Psi_{PM} \cdot i_q + (L_d - L_q) \cdot i_d \cdot i_q) \cdot \omega \cdot 3 \quad (6.2)$$

From the parameters of machine we know:

$$pp = 4$$

$$\Psi_{PM} = 0,1883 \text{ Wb}$$

We need to calculate the i_d and i_q current through the d-q axis reciprocal circuits of the machine and for that we need to transfer U_i voltage to d-q axis. According to Park's transformation we calculated the direct and quadrature part of U_i . We calculated this transformation only for one phase and that's the reason why we need to multiply equation 6.2 with number 3.

$$U_{ia} = 59,65V \text{ (amp)}$$

$$U_{ic} = U_{ib} = 0 \text{ V}$$

$$U_{id} = \frac{2}{3} \cos(0)U_{ia} + \frac{2}{3} \cos(-120^\circ)U_{ib} + \frac{2}{3} \cos(120^\circ)U_{ic} = \frac{2}{3} \cos(0)U_{ia} = 39,766V$$

$$U_{iq} = -\frac{2}{3} \sin(0)U_{ia} - \frac{2}{3} \sin(-120^\circ)U_{ib} - \frac{2}{3} \sin(120^\circ)U_{ic} = -\frac{2}{3} \sin(0)U_{ia} = 0V$$

From this transformation we can see that voltage U_{id} is cosinus shaped with amplitude 39,766V and U_{iq} is sinus shaped with amplitude 39,766V (28,118Vrms) with phase shift 90°.

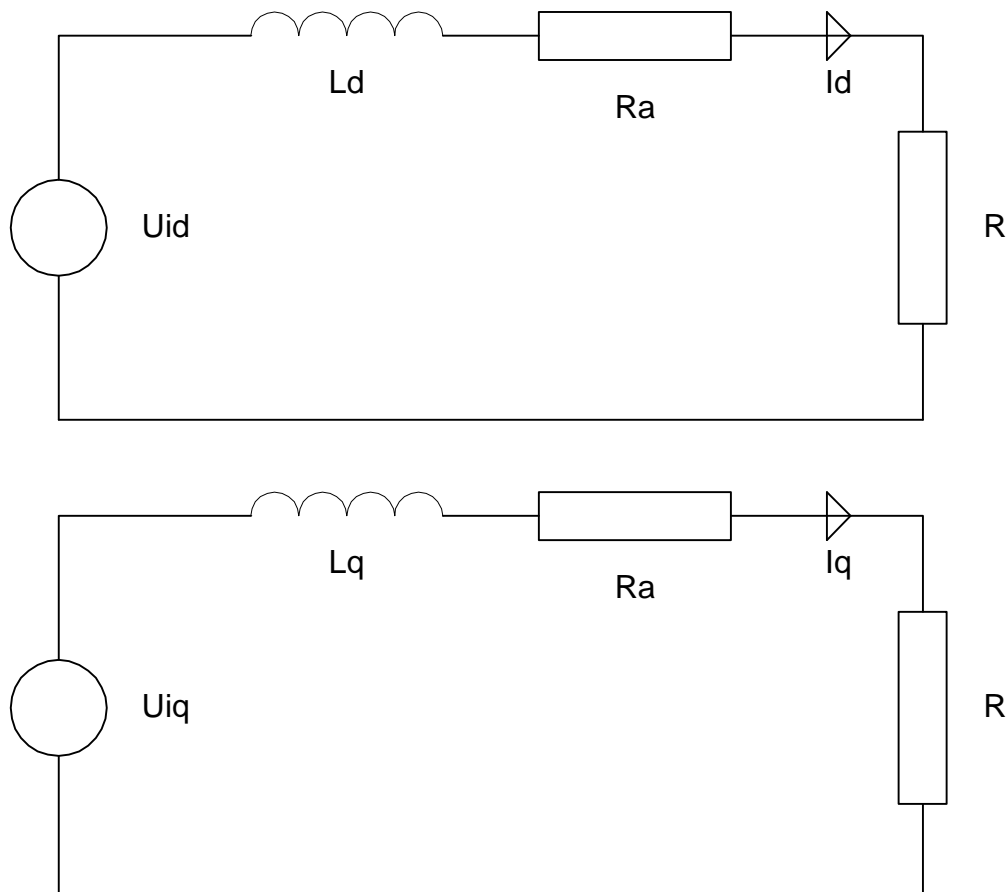


Fig. 40. Reciprocal circuits in d-q axis.

We calculated I_d and I_q currents and the load resistor R is same as we calculated before (Fig.38.).

$$Id = \frac{Uid}{\omega \cdot Ld + Ra + R} = \frac{28,118}{2 \cdot \pi \cdot 21,667 \cdot 0,0003268 + 0,0281 + 0,1344} = 135,84A$$

$$Iq = \frac{Uiq}{\omega \cdot Lq + Ra + R} = \frac{28,118}{2 \cdot \pi \cdot 21,667 \cdot 0,0006089 + 0,0281 + 0,1344} = 114,58A$$

Then we calculated power of machine according to the change of load angle β .

$$P = 1,5 \cdot 4 \cdot (0,1883 \cdot \sqrt{2} \cdot 114,58 \cdot \sin \beta + (0,0003268 - 0,0006089) \sqrt{2} \cdot 135,84 \cos \beta \cdot \sqrt{2} \cdot 114,58 \cdot \sin \beta) \cdot 2 \cdot \pi \cdot 23,333$$

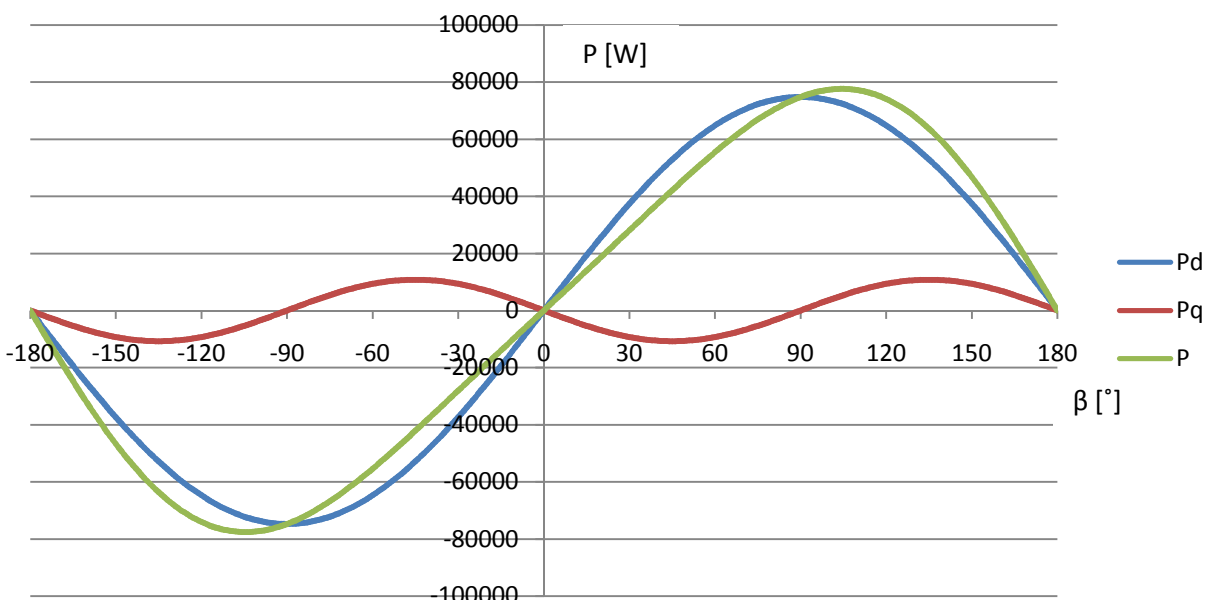


Fig. 41. Power characteristic of the synchronous machine according to load angle from second equation.

Nominal power of machine from second equation is:

$$P_{nom} = \frac{\int_{0^\circ}^{180^\circ} P d\beta}{180} = 47598,6W$$

The power characteristics from both equations are very similar and for better comparison we put them in one characteristics (Fig. 42.). The nominal given machine power is 45kW and in our results from the equations we get 49,5kW and 47,6kW which is slightly higher than nominal value and from this we can assume that our results are correct. Also from the characteristics we can see that nominal power is around load angle $\beta = 50^\circ$.

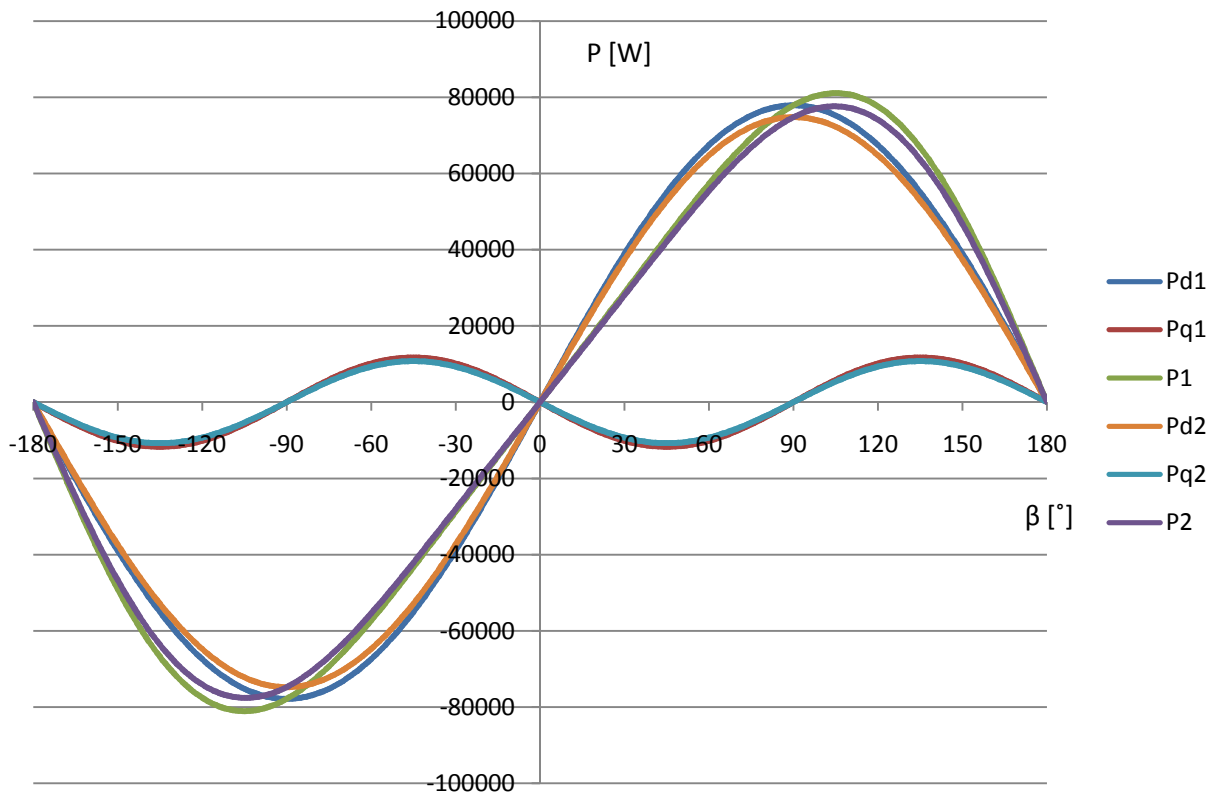


Fig. 42. Power characteristic of the synchronous machine according to load angle from both equations.

At least we calculated torque characteristics from the first equation by simple dividing of power P with angular velocity ω (Fig. 43.).

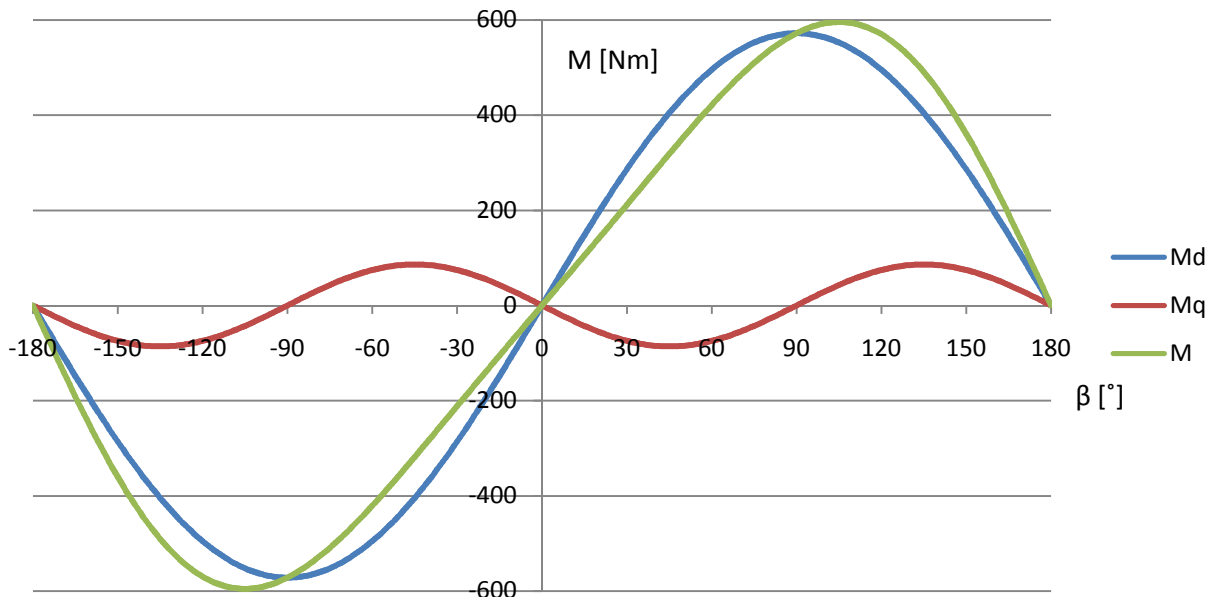


Fig. 43. Torque characteristic of the synchronous machine according to load angle from first equation.

Nominal torque of machine from first equation is:

$$M_{nom} = \frac{\int_{0^\circ}^{180^\circ} M d\beta}{180} = 364 \text{ Nm}$$



7 CONCLUSION

By using the proposed method of capacitance/reluctance network firstly we created a static model of the synchronous PM machine with linear magnetic resistors. The shape of the resulting magnetic flux density in the air gap was correct but the value of density is higher than in the real machine. In the continuation of this work we replaced the linear magnetic resistors with nonlinear corresponding to the BH curve of the used steel sheets. We compared our results with the FEM method calculated values. Then we made a dynamic parametric simulation from which we calculated induced voltage in one coil of the winding. At the end we calculated power and torque characteristics using induced voltage and reciprocal circuits of machine and two methods of calculation. The calculated nominal values of power correspond to the nominal values of this motor.



REFERENCES

- [1] Androlio,M. Bertoncelli,T. Di Gerlando,A.: A Magnetic Network Approach to the Transient Analysis of Synchronous Machines. Milano. Article.
- [2] Chmelíček,P.: FEM calculation of inductances for salient PM machine. Brno:2009. Article.
- [3] Gieras,J.F. Wing,M.: PERMANENT MAGNET MOTOR TECHNOLOGY. New York. ISBN 0-8247-0739-7.
- [3] Göl,O. Sobhi-Najafabadi,B.: A General Approach to the Dynamic Modelling of Permanent Magnet Machines. Mawson Lakes. Article.
- [4] Haydock, L. MacDonald,D.C.: A DETAILED LUMPED-PARAMETER METHOD FOR THE STUDY OF ELECTRICAL MACHINES IN TRANSIENT STABILITY STUDIES . London. Article.
- [5] Ida, N. Bastos,J.P.A.: Electromagnetics and Calculation of Fields. New York:1992, ISBN 0-387-97852-6.
- [6] Nakamura,K. Kimura,K. Ichinokura,O.: Electromagnetic and motion-coupled analysis for switched reluctance motor based on reluctance network analysis. Sendai:2004. Article.
- [7] Pyrhönen,J. Jokinen,T. Hrabcová,V.: Design of Rotating Electrical Machines. 2008, ISBN 974-0-470-69516-6.



ENCLOSURE

Datasheet of used PM manufactured by MagnetUK:

Grade	(BH)max kJm ⁻³	Br MGOe	Br mT	bHc Gauss	bHc kAm ⁻¹	Hc Oe	Hc kAm ⁻¹	Oe	Permeability	Density gr/cc	Max op temp °C	Curie temp. °C
N33	255	32	1150	11500	? 836	? 10500	? 955	? 12000	1.05	7.3	80	~ 320
N33SH	259	32.5	1150	11500	844	10600	1592	20000	1.05	7.3	150	~ 320
N33EH	259	32.5	1150	11500	836	10500	2388	30000	1.05	7.3	200	~ 320
N35	275	34.5	1195	11950	868	10900	955	12000	1.05	7.3	80	~ 320
N35SH	275	34.5	1195	11950	876	11000	1592	20000	1.05	7.3	150	~ 320
N35EH	275	34.5	1195	11950	876	11000	2388	30000	1.05	7.3	200	~ 320
N38	298.5	37.5	1235	12350	899	11300	955	12000	1.05	7.3	80	~ 320
N38SH	298.5	37.5	1235	12350	907	11400	1592	20000	1.05	7.3	150	~ 320
N38EH	298.5	37.5	1235	12350	899	11300	2388	30000	1.05	7.3	200	~ 320
N40	314	39.5	1265	12650	907	11400	955	12000	1.05	7.3	80	~ 320
N40H	314	39.5	1265	12650	923	11600	1353	17000	1.05	7.3	120	~ 320
N40SH	314	39.5	1265	12650	939	11800	1592	20000	1.05	7.3	150	~ 320
N42	330	41.5	1300	13000	915	11500	955	12000	1.05	7.3	80	~ 320
N42H	330	41.5	1300	13000	955	12000	1353	17000	1.05	7.3	120	~ 320
N42SH	330	41.5	1300	13000	987	12400	1592	20000	1.05	7.3	150	~ 320
N45	354	44.5	1350	13500	923	11600	955	12000	1.05	7.3	80	~ 320
N45M	354	44.5	1350	13500	995	12500	1114	14000	1.05	7.3	100	~ 320
N45H	354	44.5	1350	13500	955	12000	1353	17000	1.05	7.3	120	~ 320
N48	378	47.5	1400	14000	923	11600	955	12000	1.05	7.3	80	~ 320
N48M	378	47.5	1395	13950	1027	12900	1114	14000	1.05	7.3	100	~ 320
N50	394	49.5	1425	14250	796	10000	876	11000	1.05	7.3	60	~ 320
N50M	394	49.5	1425	14250	1033	13000	1114	14000	1.05	7.3	100	~ 320

BH curve of used electrical steel sheets:

M235-35A SURA ELECTRICAL STEEL BH CURVE

B [T]	H [A/m]
0.1	25
0.2	33
0.3	38
0.4	44
0.5	48
0.6	55
0.7	62
0.8	72
0.9	83
1	100
1.1	125
1.2	170
1.3	280
1.4	680
1.5	1800
1.6	4000
1.7	7000
1.8	12000
1.9	20000
2	30000



Chart of the values of magnetic flux density in the air gap depending on the current (Fig. 19.):

$\theta [^{\circ}]$	B [T]				
	I=0A	I=17,505A	I=35,01A	I=52,52A	I=70,02A
0	0,036	0,029	0,022	0,015	0,008
1,5	0,036	0,029	0,022	0,015	0,008
3	0,036	0,029	0,022	0,015	0,008
4,5	0,036	0,029	0,022	0,015	0,008
6	0,036	0,029	0,022	0,015	0,008
7,5	0,009	0,025	0,041	0,056	0,072
9	0,85	0,836	0,822	0,809	0,795
10,5	0,85	0,836	0,822	0,809	0,795
12	0,85	0,836	0,822	0,809	0,795
13,5	0,85	0,836	0,822	0,809	0,795
15	0,16	0,167	0,173	0,179	0,185
16,5	1,5	1,564	1,634	1,704	1,774
18	1,5	1,564	1,634	1,704	1,774
19,5	1,5	1,564	1,634	1,704	1,774
21	1,5	1,564	1,634	1,704	1,774
22,5	0,278	0,299	0,321	0,343	0,365
24	1,5	1,666	1,833	1,998	2,165
25,5	1,5	1,666	1,833	1,998	2,165
27	1,5	1,666	1,833	1,998	2,165
28,5	1,5	1,666	1,833	1,998	2,165
30	0,275	0,297	0,319	0,340	0,362
31,5	0,864	0,906	0,948	0,990	1,032
33	0,864	0,906	0,948	0,990	1,032
34,5	0,864	0,906	0,948	0,990	1,032
36	0,864	0,906	0,948	0,990	1,032
37,5	0,156	0,155	0,154	0,154	0,153
39	0,045	0,106	0,166	0,227	0,288
40,5	0,045	0,106	0,166	0,227	0,288
42	0,045	0,106	0,166	0,227	0,288
43,5	0,045	0,106	0,166	0,227	0,288
45	0,007	0,001	0,005	0,011	0,017